Received: 31 August 2022 | Revised: 27 October 2022 | Accepted: 29 October 2022

DOI: 10.1002/bdd.2338

WILEY

INVITED REVIEW

Biodistribution and delivery of oligonucleotide therapeutics to the central nervous system: Advances, challenges, and future perspectives

Akihiko Goto | Syunsuke Yamamoto | Shinji Iwasaki

Drug Metabolism and Pharmacokinetics Research Laboratories, Preclinical and Translational Sciences, Research, Takeda Pharmaceutical Company Limited, Fujisawa, Kanagawa, Japan

Correspondence
Shinji Iwasaki, 26-1, Muraoka-Higashi 2-chome, Fujisawa, Kanagawa 251-8555, Japan.
Email: shinji.iwasaki@takeda.com

Abstract

Considerable advances have been made in the research and development of oligonucleotide therapeutics (OTs) for treating central nervous system (CNS) diseases, such as psychiatric and neurodegenerative disorders, because of their promising mode of action. However, due to the tight barrier function and complex physiological structure of the CNS, the efficient delivery of OTs to target the brain has been a major challenge, and intensive efforts have been made to overcome this limitation. In this review, we summarize the representative methodologies and current knowledge of biodistribution, along with the pharmacokinetic/pharmacodynamic (PK/PD) relationship of OTs in the CNS, which are critical elements for the successful development of OTs for CNS diseases. First, quantitative bioanalysis methods and imaging-based approaches for the evaluation of OT biodistribution are summarized. Next, information available on the biodistribution profile, distribution pathways, quantitative PK/PD modeling, and simulation of OTs following intrathecal or intracerebroventricular administration are reviewed. Finally, the latest knowledge on the drug delivery systems to the brain via intranasal or systemic administration as noninvasive routes for improved patient quality of life is reviewed. The aim of this review is to enrich research on the successful development of OTs by clarifying OT distribution profiles and pathways to the target brain regions or cells, and by identifying points that need further investigation for a mechanistic approach to generate efficient OTs.

KEYWORDS
biodistribution, central nervous systems, drug delivery system, oligonucleotide therapeutics

Akihiko Goto, Syunsuke Yamamoto, and Shinji Iwasaki equally contributed to the preparation of this manuscript.

1 | INTRODUCTION

The development of oligonucleotide therapeutics (OTs), including antisense oligonucleotides (ASOs) and small interfering RNA (siRNA), has been remarkable in terms of therapy for diseases that cannot be treated with traditional medications. OTs have provided a treatment option for various diseases, such as givosiran for acute hepatic porphyria and inotersen for familial amyloidosis (Dohrn et al., 2021; Syed, 2021). Central nervous system (CNS) diseases are often inherited or caused by the accumulation of pathogenic proteins. Traditional drugs often provide limited options to treat CNS diseases due to the difficulties in pathological protein reduction. Contrarily, OTs could be an effective treatment modality to act on causative genes by the modification of target mRNA expression. Numerous OTs have being developed, such as those targeting the genes *microtubule-associated protein tau* (*MAPT*) for Alzheimer's disease, *huntingtin* (*HTT*) for Huntington's disease, and *superoxide dismutase 1* (*SOD1*) for amyotrophic lateral sclerosis (Crooke et al., 2021; DeVos et al., 2017; Miller et al., 2013, 2022; Tabrizi et al., 2019). Here we summarize the approved and clinically investigating OTs for CNS disease as of September 2022 in Table 1. Only nusinersen has been launched already as OTs to CNS. However, there are several OTs in the late stage; hence, some OTs would be submitted to new drug applications soon if a pivotal clinical study successfully reveals the effect of treatment. As for the OTs modality in the clinical stage, most candidates are ASOs-based, and only ALN-APP is of the siRNA basis. Regarding the root of administration (ROA), intrathecal (IT) dosing is the only ROA investigated currently.

Because the efficient delivery of OTs to target brain cells is critical to the successful development of OTs for CNS disease, various studies have been conducted on the brain distribution profile of OTs. This review first summarizes methodologies to evaluate the biodistribution of OTs in the brain. Second, the biodistribution of OTs following IT or intracerebroventricular (ICV) administration, the commonly used ROA, is reviewed in terms of the points and pathways of brain distribution and quantitative pharmacokinetic/pharmacodynamic (PK/PD) analysis. Third, investigations into intranasal or systemic drug delivery systems (DDSs) aiming to mitigate the

TABLE 1 Summary of the CNS-targeted OTs launched and under clinical development as of September 2022

Name	Modality	Indication	Target	Route of administration	Development stage	ClinicalTrials.gov identifier
Nusinersen	ASO	SMA	SMN2	IT	Launched	NCT02462579
Tofersen	ASO	ALS	SOD1	IT	Phase 3	NCT02623699
ION363	ASO	ALS	FUS	IT	Phase 3	NCT04768972
Zilganersen	ASO	AxD	GFAP	IT	Phase 3	NCT04849741
Tominersen	ASO	HD	HTT	IT	Phase 3	NCT03842969
IONIS-MAPTRx/ BIIB080	ASO	AD, FTD	MAPT	IT	Phase 2	NCT05399888
ION859/BIIB094	ASO	PD	LRRK2	IT	Phase 2	NCT03976349
STK-001	ASO	DS	SCN1A	IT	Phase 2	NCT04740476
GTX-102	ASO	AS	UBE3A-ATS	IT	Phase 1/2	NCT04259281
ION582	ASO	AS	UBE3A-ATS	IT	Phase 1/2	NCT05127226
WVE-003	ASO	HD	HTT	IT	Phase 1/2	NCT05032196
WVE-004	ASO	ALS, FTD	C9orf72	IT	Phase 1/2	NCT04931862
ION541/BIIB105	ASO	ALS	ATXN2	IT	Phase 1	NCT04494256
ION260/BIIB132	ASO	SAT3	ATXN3	IT	Phase 1	NCT05160558
ION464/BIIB101	ASO	MSA, PD	SNCA	IT	Phase 1	NCT04165486
ALN-APP	siRNA	AD, CAA	APP	IT	Phase 1	NCT05231785

Abbreviations: AD, Alzheimer's disease; ALS, amyotrophic lateral sclerosis; APP, amyloid precursor protein; AS, Angelman syndrome; ASO, antisense oligonucleotide; ATXN, ataxin; AxD, Alexander disease; C9orf72, chromosome 9 open reading frame 72; CAA, cerebral amyloid angiopathy; CNS, central nervous system; DS, Dravet syndrome; FTD, frontotemporal degeneration; FUS, fused in sarcoma; GFAP, glial fibrillary acidic protein; HD, Huntington's disease; HTT, huntingtin; IT, intrathecal; LRRK, leucine-rich repeat kinase; MAPT, microtubule-associated protein tau; MSA, multiple system atrophy; OT, oligonucleotide therapeutics; PD, Parkinson's disease; SAT3, spinocerebellar ataxia type 3; SCN1A, sodium voltage-gated channel alpha subunit 1; SMA, spinal muscular atrophy; SMN2, survival motor neuron 2; SNCA, synuclein alpha; SOD1, superoxide dismutase 1; UBE3A-ATS, ubiquitin protein ligase E3A-antisense transcript.

invasiveness of IT and ICV administration are summarized. This review describes the current status and future perspectives of these topics. Through this review, we aim to promote research for OT delivery to the CNS and its quantitative translation to humans.

2 | IT AND ICV ADMINISTRATION AS THE CURRENT GOLD STANDARD APPROACH

This section summarizes the distribution profiles after IT and ICV administration and the bioanalytical methods for analyzing their distribution.

2.1 | Methodology to evaluate brain distribution

Understanding bioanalysis methods is essential to assess the biodistribution of OTs in the brain. Two main approaches have been employed to assess the brain distribution of OTs: concentration measurement and imaging of the region of interest (Tables 2 and 3).

Quantitative measurement of OT concentrations in brain regions such as the cerebral cortex and hippocampus has been performed to assess brain drug distribution (Jafar-Nejad et al., 2021; Mazur et al., 2019). Hybridization enzyme-linked immunosorbent assay (HELISA) is widely used for pharmacokinetic evaluation (Mazur et al., 2019; Shi et al., 2021; Valenzuela et al., 2021). HELISA is a highly sensitive method and does not require expensive equipment or specific extraction techniques, despite concerns about cross-reactivity with metabolites (Chan et al., 2010; Yu et al., 2002). In a study by Wei et al. (2006) the target nucleic acid was captured using a capture probe with sequences complementary to those of the analyte and detection probe. After the detection probe was ligated to the analyte on the capture probe, the single-stranded moiety of the capture probe was cleaved with S1 nuclease; subsequently, fluorescence measurement was performed on digoxigenin bound to the detection probe using an alkaline phosphatase system. The authors found 78% cross-reactivity, with a metabolite shorter by one base at the 5′-end (Wei et al., 2006). Such cross-reactivity may be reduced by using a probe with a higher affinity for the target analyte, such as locked nucleic acid (LNA) probes (Thayer et al., 2019). Additionally, the detection sensitivity can be enhanced by amplifying signals using branched DNA technology (Mahajan et al., 2022). Moreover, a wider dynamic range can be obtained by changing the detection system from a standard fluorescent plate reader to an electrochemiluminescence platform developed by Meso Scale Discovery (MSD; Rockville, MD, USA) (Thayer et al., 2019).

Drug concentration measurement using liquid chromatography-tandem mass spectrometry (LC-MS/MS) is also used to quantify OTs (Nuckowski et al., 2018; Shi et al., 2021; Zhang et al., 2007). LC-MS/MS is advantageous because of its excellent specificity, selectivity, and applicability to various modifications and sequences (Studzinska, 2018). However, disadvantages of the assay include the need for expensive equipment and expertise, relatively low sensitivity, and complicated sample preparation such as liquid–liquid or solid-phase extraction (Lin et al., 2007). Hybridization–LC-MS/MS, which uses a capture probe to extract the analyte (nucleic acid) from the sample, as is the case with HELISA, is more useful to avoid issues with sensitivity and preparation procedures. The application of this method is expected to increase in the future (Li et al., 2020).

Quantitative polymerase chain reaction (PCR) using reverse transcription techniques based on tailed primers, stem-loop primers, or adapter addition provides high sensitivity and a wide dynamic range. However, it raises concerns about specificity and selectivity, as well as variations in reverse transcription and PCR efficiencies (Cheng et al., 2009; Duncan et al., 2006; Landesman et al., 2010; Shi et al., 2012; Stratford et al., 2008; Zhang et al., 2011). Since all these quantitative systems possess advantages and disadvantages, it is vital to use them appropriately according to the study objectives (Table 2).

Here we propose the microenvironmental pharmacokinetic analysis (μPK analysis) of OTs. Since the tissue distribution and intracellular disposition of OTs are nonuniform, the concentration in the whole-brain homogenate might provide misleading insights into the brain distribution because it may not represent the concentration at the targeted region, cell type, and organelle. PK/PD evaluation of OTs targeting cell type–specific mRNA includes the qualitative estimation of the distribution to target cells by the knockdown effect. However, it is difficult to evaluate the brain distribution based on the

TABLE 2 Summary of the quantification methodologies for the evaluation of OT distribution in the brain

Assay modality	HELISA	LC-MSMS	qPCR
Sensitivity	High	Middle	High
Dynamic range	Narrow to middle	Middle	Wide
Specificity/selectivity	Potentially cross-reactive to metabolites and endogenous sequences	High	Potentially cross-reactive to metabolites
Sample preparation	Sample dilution and hybridization-based extraction using specific probes	Complicated sample preparation, such as liquid–liquid or solid-phase extraction	Complicated sample preparation, such as liquid–liquid or solid-phase extraction

Abbreviations: HELISA, hybridization enzyme-linked immunosorbent assay; LC-MS/MS, liquid chromatography-tandem mass spectrometry; OT, oligonucleotide therapeutics; qPCR, quantitative polymerase chain reaction.

TABLE 3 Summary of imaging methodologies for the evaluation of brain distribution of OTs

Imaging modality	PET/SPECT	In vivo confocal/multiphoton microscopy	CFT	LSFM	Microscopy of tissue slice	Imaging MS
Observation range	Whole body	Tissue surface	Whole body to tissue	Whole body to tissue	Tissue section	Tissue section
Invasive	In life	Tissue exposure	Tissue sampling	Tissue sampling	Tissue sampling	Tissue sampling
Period	Short to long term	Short term	Snapshot	Snapshot	Snapshot	Snapshot
Resolution	Low (typically submillimeter range)	Cellular to subcellular	Cellular to subcellular	Cellular	Subcellular	Cellular to subcellular
Labeling	Predosing	Predosing	Predosing	Predosing or after sampling	Predosing or after sampling	Predosing or after sampling or label-free
Observation of OTs in fluid	Possible	Possible	Possible	Impossible	Impossible	Impossible

Abbreviations: CFT, cryo-fluorescence tomography; LSFM, light sheet fluorescence microscopy; MS, mass spectrometry; OTs, oligonucleotide therapeutics; PET, positron emission tomography; SPECT, single photon emission computed tomography.

knockdown effect when performing PK/PD evaluation of OTs targeting ubiquitously expressed mRNAs, such as metastasis associated in lung adenocarcinoma transcript-1 (Malat1). Moreover, PK/PD evaluation at the site of action would contribute to efficient molecular design and translation to human PK/PD. Therefore, it is necessary to quantify OTs in the target cells to evaluate the distribution in the brain. Although single-cell isolation technologies such as fluorescence-activated cell sorting (FACS), magnetic-activated cell sorting, and laser capture microdissection have been developed (Hu et al., 2016); to the best of our knowledge, no reports of quantitative detection of drug levels in target brain cells have been made. This should be considered as a future application in OT distribution studies. Furthermore, the evaluation clarifies how much OTs are required to reduce the target mRNA by quantifying OTs contained in specific intracellular components. Although ASOs in the nucleus and cell fractions from Hela cells have been quantified (Pendergraff et al., 2020), reports of the organelle isolation from in vivo samples for OT distribution analysis are limited. Nott et al. (2021) successfully isolated nuclei derived from various cells of a mouse brain using FACS. The extraction methodology would apply to the μPK analysis of OTs in the future. The evaluation of PK/PD correlation of siRNA involves the isolation and measurement of siRNA contained in the RNA-induced silencing complex by immunoprecipitation (Chong et al., 2021). The quantitative drug distribution assessment in the microenvironment through the isolation of target cells and intracellular components would represent an effective approach to PK/PD correlation analysis and proof-of-concept (POC) acquisition. For μPK analysis, a more sensitive and quantitative detection method is expected to be developed.

Imaging technology also provides a valuable tool to quantitatively or semiquantitatively assess the μPK of OTs in the brain (Mazur et al., 2019). Two main imaging techniques are available. The first is real-time three-dimensional (3D) imaging of labeled nucleic acids using techniques such as positron emission tomography (PET), single-photon emission computed tomography (SPECT), and in vivo confocal/multiple photon microscopy. The second is two-dimensional (2D) snapshots to detect signals from labeled nucleic acids in tissue sections or those stained by immunohistochemistry (IHC) or in situ hybridization (ISH) (Table 3).

PET and SPECT are excellent because the concentrations of radiolabeled ASOs after administration to animals can be measured quantitatively over time; these techniques allow the assessment of their distribution even in the body and the brain (Mazur et al., 2019). However, they are disadvantageous because they require special laboratories and have low spatial resolution. In vivo confocal/multiple photon microscopy has excellent spatial resolution and can trace the OT behavior in the microenvironment (Nagata et al., 2021); however, it has several disadvantages: the organs need to be exposed, and only the surface can be observed. These real-time 3D imaging techniques are effective for analyzing the distribution from cerebrospinal fluid (CSF) to the brain parenchyma because of their ability to observe OTs in body fluids such as CSF and interstitial fluid (ISF), which is otherwise impossible with 2D imaging.

For 2D snapshot imaging, IHC- or ISH-based methods, which allow the imaging of unlabeled nucleic acids, have often been used. IHC uses antibodies to the modified backbone and allows easy detection of unlabeled nucleic acids, although the specificity of the antibody needs to be thoroughly verified (Ait Benichou et al., 2022; Korobeynikov et al., 2022; Mazur et al., 2019; Nagata et al., 2021). In ISH, designing a probe with a strand complementary to the target nucleic acid allows relatively simple detection, and the affinity of the probe can be enhanced by modifying it suitably (e.g. LNA probe) (Goebl et al., 2007; Zhang et al., 2021). Microscopic examination of labeled nucleic acids in sections has also been widely applied and is advantageous, as it allows the assessment of drug distribution at a high resolution (Kuwahara et al., 2018). However, analysis of the tissue sections warrants attention to differences in the morphology of the target tissue between in vivo and ex vivo imaging (Mestre et al., 2020). Additionally, this technique has the disadvantages of being based on snapshots and being analyzed in a localized area.

As an application example of assay modality other than microscopic observation, He et al. (2021) reported that ASOs labeled with 5-bromo-2′-deoxythymidine in liver sections could be detected at high resolution using nanoscale secondary ion mass spectrometry (NanoSIMS). The authors successfully analyzed differences in ASO distribution among liver cell types and subcellular ASO localization. Therefore, this approach has the potential to assess nucleic acid distribution in the brain. Although the application of imaging technology using MS (MS imaging) other than NanoSIMS to the distribution evaluation of OTs is limited, there is a possibility of OTs being observed label-free. Further technological development is expected in the future.

With cryofluorescence tomography (CFT), serial imaging of frozen section surfaces allows 3D reconstruction of the organ or whole body at a high resolution; practical applications of this technique are projected to grow in the future (Mazur et al., 2019). In addition, tissue clearing technology has also been developed for the brains of mice, rats, and marmosets (Ueda et al., 2020). This technique enables comprehensive and rapid observation of the whole brain at single-cell resolution. Although there are no examples of brain distribution evaluation of OTs, it is a promising technology for studying the distribution of OTs.

As described above, OT imaging can provide many options; therefore, these techniques need to be used appropriately, according to the study purpose. Combining two or more assay modalities can compensate for their respective disadvantages.

2.2 | Brain distribution after IT/ICV administration

IT or ICV administration is a valuable ROA that delivers OTs to CNS tissues without passing through the blood–brain barrier (BBB). However, the delivered OTs are not always distributed uniformly in the brain because of their complex biology and distribution properties. This section summarizes the distribution profile of OTs after IT/ICV administration (Table 4).

Before the distribution profile of OTs is summarized, the kinetics of substances other than OTs in CSF after IT administration is introduced for a better interpretation of the dependency of substances' physicochemical properties on CSF for CNS tissue distribution (Wolf et al., 2016). It highly depends on several factors, such as molecular weight, protein, and tissue-binding properties. ^{123}I-labeled human serum albumin (HSA) reaches the cisterna magna, ventral brain, and pituitary recess 2 h after IT administration. Wolf et al. (2016) showed that the small-molecule tracer ^{111}In-diethylenetriamine-pentaacetic acid (DTPA) gets eliminated peripherally from the IT space 15 min postdose. ^{99}mTc-dimercaptosuccinic acid (DMSA), which has a higher binding affinity to HSA than that of ^{111}In-DTPA, showed more prolonged retention in the IT space, suggesting that protein binding is an impactful factor for elimination from CSF. ^{99}mTc-sestamibi with high tissue binding was trapped near the injection site, showing that the kinetics in CSF varies depending on compound physicochemical properties. Further, the regions to which ^{123}I-HSA was delivered differed greatly, depending on dosing volume, suggesting that the dosing conditions also influence distribution in CSF. Using various imaging modalities, Mazur et al. (2019) assessed the CSF distribution of ASOs after IT administration to rats. ASOs were rapidly distributed in the IT space after dosing; their distribution in CNS tissue was detected from 1 to 4 h postdose, and their clearance to peripheral tissues occurred 4 h postdose. Strong ASO signals colocalized with α-SMA, a vascular smooth muscle marker, and Reca1, an endothelial marker; ASOs were suggested to be abundant in the perivascular space. At early timepoints after administration, ASOs were highly distributed around the surface of the brain and circle of Willis; the signals then moved to the cellular side from 2 to 8 h postdose. Signals in the deep brain regions, including the striatum, were weak but dose-dependent, as in the cortex.

In a study on nonhuman primates (NHPs), different dose volumes were associated with delivered ASOs amounts to the brain (Sullivan et al., 2020). The gene knockdown levels induced by the delivered ASOs were also dose volume-dependent. Additionally, the exogenous mechanical force (thoracic percussive treatment) increased the amount of ASOs distributed in the brain.

Following IT administration of the ASOs to rats, their levels were lower in the striatum than in other brain regions, with gene knockdown levels also being lower in the striatum (Jafar-Nejad et al., 2021). A similar trend was observed in NHPs, with the levels of ASOs and gene knockdown being lower in the caudate and putamen. These results suggested that the ASOs administered by the IT route were transported against the CSF bulk flow from the ventricle to the cisterna magna (Figure 1), resulting in the low distribution in the distal, deep regions of the brain. In NHPs, ICV administration of divalent siRNA (di-siRNA) also resulted in low drug concentration and weak target gene knockdown levels in the deep brain (Alterman et al., 2019). Di-siRNA is a dimer of two siRNAs covalently connected at the 3′ ends of the sense strand through a tetraethylene glycol linker.

Following IT and ICV administration of di-siRNA to a larger animal (sheep), low distribution to the deep brain was observed via both ROAs (Ferguson et al., 2021). Contrarily, uniform distribution of

TABLE 4 Summary of the biodistribution profile of OTs following IT or ICV administration

Modality	Study condition	Detection	Key output	Reference
^{123}I-HSA, ^{111}In-DTPA, ^{99m}Tc-DMSA, ^{99m}Tc-sestamibi, $^{99m}TcO_4$	Rat: IT (10, 50 μl)	SPECT-CT	Molecular weight, protein binding, tissue binding, and dosing volume effect on the distribution and elimination profile	Wolf et al. (2016)
(^{125}I or Cy7) ASO	Rat: IT (30 μl)	SPECT-CT IHC CFT Fluorescence microscopy	Rapid distribution to the CSF space (−1 h) followed by CNS tissue distribution (1–4 h) and elimination to peripheral tissues (from 4 h) Strong signal around the perivascular space Low signal in the deep brain	Mazur et al. (2019)
^{64}Cu-DOTA, ^{99m}Tc-DTPA w/ASO, ASO	NHP: IT (0.8 ml, 2.0 ml)	PET/SPECT-CT LC-MS IHC	Dosing volume–dependent distribution and knockdown efficiency Convective force alters the distribution distance from injection site	Sullivan et al. (2020)
ASO	Mouse: ICV (10 μl) Rat: IT (30 μl) NHP: IT (1 ml)	HELISA IHC	Homogeneous distribution in mouse ICV Heterogeneous distribution (low conc. in deeper brain) in rat and NHP IT, with consistent knockdown effect Cell type difference on dose-knockdown efficiency after mouse ICV	Jafar-Nejad et al. (2021)
mono/di-siRNA (with/without Cy3)	Mouse: IS (2 μl), ICV (5 μl/site) NHP: ICV (0.75 ml)	Fluorescence microscopy LC/MS	Wider and higher distribution of di-siRNA than mono-siRNA High concentration in the deep brain but low in the medial cortex in mouse ICV Heterogeneous distribution in NHP ICV, with consistent protein silencing effect	Alterman et al. (2019)
di-siRNA (with/without Cy3)	Mouse: ICV (5 μl/site), IT (10 μl) Sheep: ICV (1.5 ml), IT (1.5 ml), IS (50 μl)	Fluorescence microscopy PNA hybridization assay	Heterogeneous distribution, low concentration in the deep brain (putamen) after ICV/IT in sheep	Ferguson et al. (2021)
C16-siRNA (with/without VP)	Rat: IT (30 μl) NHP: IT (2.0 ml)	IHC LC-MS	C16- and VP-incorporated siRNA showed wider distribution and stronger distribution than naked siRNA May not reach the deep brain (striatum)	Brown et al. (2022)

Abbreviations: ASO, antisense oligonucleotide; C16, 2′-O-hexadecyl; CFT, cryo-fluorescence tomography; CNS, central nervous system; CSF, cerebrospinal fluid; di-siRNA, divalent small interfering RNA; DMSA, dimercaptosuccinic acid; DOTA, dodecane tetraacetic acid; DTPA, diethylenetriamine pentaacetic acid; HELISA, hybridization enzyme-linked immunosorbent assay; HSA, human serum albumin; ICV, intracerebroventricular; IHC, immunohistochemistry; IT, intrathecal; LC-MS, liquid chromatography-tandem mass spectrometry; NHP, nonhuman primate; OTs, oligonucleotide therapeutics; PET, positron emission tomography; PNA, peptide nucleic acid; SPECT-CT, single-photon emission computed tomography-computed tomography; VP, 5′-(E)-vinylphosphonate.

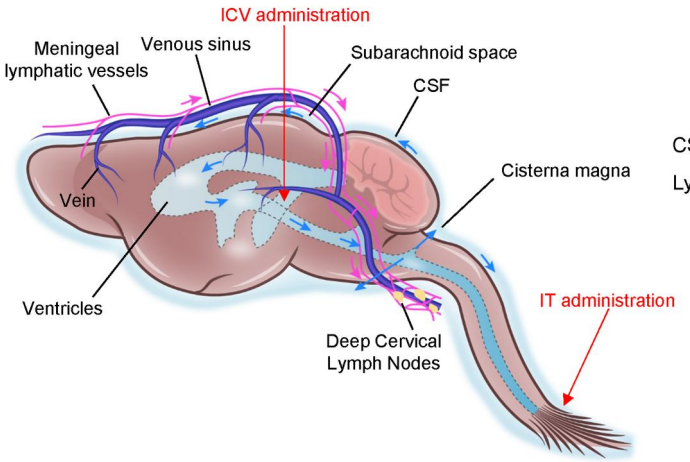

FIGURE 1 Cerebrospinal fluid (CSF) and lymphatic flow in rodents. CSF is produced at the choroid plexus of the ventricles, transported into the subarachnoid space at the cisterna magna, and then distributed around the brain. Lymphatic vessels are located parallel to the dural venous sinuses and are connected to the lymph node

ASOs in the brain and knockdown of target genes was observed in mice receiving ICV administration (Jafar-Nejad et al., 2021). In the case of di-siRNA ICV dosing to mice, distribution into the striatum is not low, while a relatively low concentration was observed in the medial cortex (Alterman et al., 2019). OT delivery to deep brain regions at levels comparable with other regions has been observed only in mouse ICV studies. Taken together, heterogeneous distribution likely occurs after IT or ICV administration in animals other than mice. Such heterogeneous distribution could be a big hurdle for the treatment of disease associated with the deep brain region following IT or ICV administration of OTs.

The relationship between gene knockdown and dose after IT administration of ASOs to NHPs was also examined in cell fractions from the cortex. The rank order of doses showing half-maximal knockdown (ED_{50}) was as follows: astrocyte (17 μg) < oligodendrocyte (34 μg) < microglia (71 μg) < neuron (206 μg); the sensitivity varied depending on the cell type (Jafar-Nejad et al., 2021). Differences in cellular uptake, intracellular distribution of ASOs, and the activity of RNase H1 might contribute to these results. For CNS disease treatment, the target cell is often specific to one cell type (e.g. Tau aggregation in neurons) (Habekost et al., 2021), and intensive distribution to nontarget cell types is inefficient. Moreover, the PK and knockdown assessment in total brain homogenate potentially cause inappropriate PK/PD analysis and translation. Consequently, cellular-level PK/PD evaluation would be quite important to generate OTs having better target cell distribution specificity and to analyze truly quantitative PK/PD analysis.

In sheep receiving a 50-mg dose of di-siRNA, an extremely high concentration (100 μg/g tissue) of di-siRNA was detected in the brain (Ferguson et al., 2021); this value was much higher than the brain di-siRNA concentration in NHPs receiving a a 25-mg dosage (approximately 10 μg/g tissue) (Alterman et al., 2019). The prolonged CSF retention attributable to the large molecular weight and charge may contribute to this high concentration. Additionally, the concentration difference between NHP and sheep could be derived from the difference in elimination from CSF, which might be associated with the CSF bulk flow rate difference (slower in sheep than in NHPs) (Fowler et al., 2020). Brown et al. (2022) found that conjugation of 2′-O-hexadecyl (C16) and 5′-(E)-vinylphosphonate to siRNA provided wider biodistribution and higher siRNA concentration after IT administration in rats and NHPs, producing a more potent therapeutic effect than nonconjugated siRNA did. In other studies (Ferguson et al., 2021; Jafar-Nejad et al., 2021), C16-conjugated siRNA concentrations were also lower in the striatum in the deep brain than in other regions, and mRNA knockdown tended to be weaker in the striatum. As with the di-siRNA case described above, the molecular weight and physicochemical properties of OTs may impact their brain distribution.

As described in this section, regional drug distribution in the brain after IT/ICV administration is being clarified, but there are still unknown factors underlying differences in distribution. The mechanistic understanding of biodistribution should provide rational approaches of lead optimization and quantitative translation to humans. Correlations of the chemical structure of the substance with brain distribution, species differences in regional distribution, and the delivery system of OTs to the deep brain region warrant further investigation. Identifying detailed distribution pathways from CSF to the brain parenchyma and elimination pathways from the brain parenchyma to peripheral tissues are crucial, not only for realizing the superior distribution of OTs even at the deep brain region, but also for the mechanism-based PK/PD translation to humans. The current understanding of these pathways is summarized in the next section.

2.3 | Pathways of distribution to the brain and drainage from the brain after IT/ICV injection

To understand the pathways for brain distribution and elimination of OTs, we need to define the glymphatic system and the intramural periarterial drainage (IPAD) pathway (Figure 2). The glymphatic system consists of the entry of CSF into the brain through the periarterial space, influx from the periarterial space into the ISF, and efflux from the ISF into the perivenous space (Evans & Smitherman, 1989) (Figure 2a,b). Using imaging technology, Iliff et al. (2012) assessed the distribution of fluorescent tracers of various molecular weights after ICV or intracisternal magna (ICM) administration. The

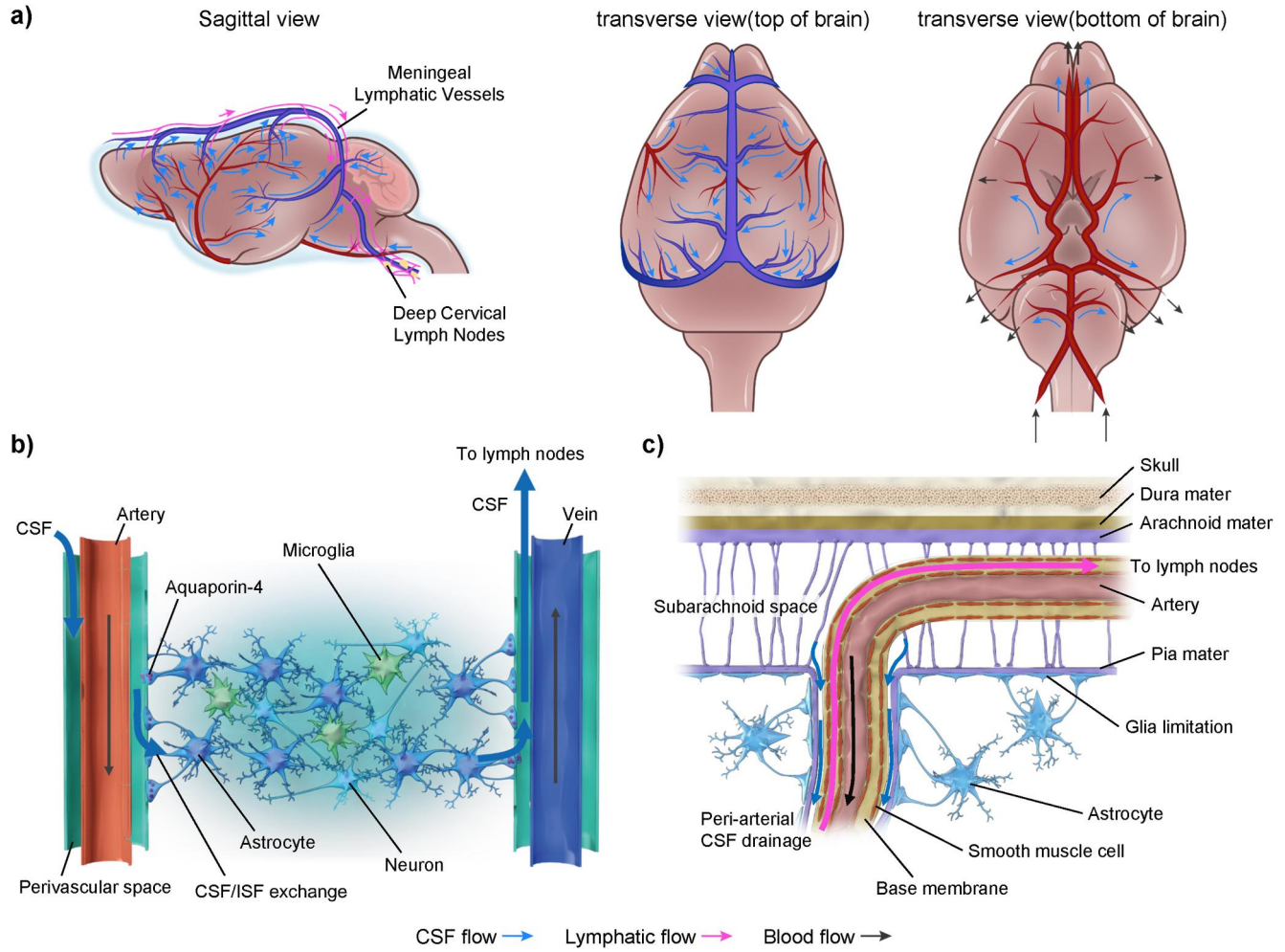

FIGURE 2 Glymphatic system and intramural periarterial drainage (IPAD). Blue, pink, and black arrows represent cerebrospinal fluid (CSF), lymphatic, and blood flow, respectively. (a) CSF flow in the perivascular space and lymphatic flow in rodents. CSF is transported into the perivascular space in the direction of blood flow. CSF and solutes would be drained into lymphatic vessels and then transported into the lymph node. (b) CSF–interstitial fluid exchange. CSF is transported into the perivascular space of arteries in the direction of blood flow, mixed with interstitial fluid (ISF), and then drained into the perivascular space of the veins. This CSF–ISF exchange is mediated by aquaporin-4 (AQP4) expressed at astrocyte endfeet. (c) IPAD pathway. ISF and solutes are drained into the base membrane of arteries in the reverse direction of blood flow and then transported into the lymph node

distribution of fluorescent tracers in the brain parenchyma via the ependyma was limited to 30 min after ICV administration, following which brain distribution of fluorescent dextran with a molecular weight of 2000 kDa along the perivascular space and its limited distribution in the interstitial space of the brain parenchyma were observed. Additionally, dextran with a molecular weight of 3 kDa, was shown to concentrate in the perivascular space and pial surface, followed by entering the interstitial space of the brain parenchyma. In vivo imaging with a two-photon microscope revealed that fluorescent dextran, after ICM administration, entered not the vein but the brain along the outside of cortical surface arteries and penetrating arteries. Finally, it was suggested that the water channel aquaporin-4 (AQP4) contributes to tracer distribution from the periarterial space to the parenchyma and that AQP4 is responsible for the influx of CSF from the periarterial space into ISF in the brain parenchyma, as well as the efflux of ISF from the brain parenchyma into the perivenous space (Figure 2b). This glymphatic CSF–ISF exchange demonstrated in mice was also confirmed in rats using magnetic resonance imaging (Iliff et al., 2013). Interestingly, sleep has been reported to enhance this glymphatic CSF–ISF exchange, and attention should be paid to anesthesia and timepoint analyses for the assessment of tracer distribution in the brain (Xie et al., 2013). The meningeal glymphatic system has been identified to serve as the downstream drainage pathway from ISF to CSF exchange in the glymphatic system, and macromolecules are cleared into the meningeal lymphatic system (Aspelund et al., 2015; Louveau et al., 2016). This lymphatic elimination occurs at a high velocity, with the tracers injected into the brain parenchyma or CSF detected in the cervical lymph nodes within several minutes after injection (Plog et al., 2015).

IPAD has been identified as a drainage pathway of ISF and solutes (Figure 2c). Szentistvanyi et al. (1984) found that the tracers injected into the brain were transported along the artery in the

direction against the blood flow and transferred to the cervical lymph nodes. This pathway was later shown to function through the base membranes located between the smooth muscle cell layers in the artery and has been proposed as a transfer pathway from the brain to the meningeal lymphatic system (Carare et al., 2014). Several studies considered pulsations to provide a power source for IPAD (Carare et al., 2008; Sharp et al., 2016). However, some studies either do not support this view (Diem et al., 2017) or consider vasomotion as a motor power (Aldea et al., 2019). Conflicting studies have debated the transfer pathway to the meningeal lymphatic system.

Mazur et al. (2019) investigated the brain distribution of ASOs after IT administration using various imaging modalities. Analysis by 3D CFT showed that ASOs were localized on the penetrating arteries, Willis' circle, and the mouse brain surface immediately after IT administration. Additionally, IHC analysis revealed that ASOs colocalized with Reca1 (a vascular endothelial marker), alpha-smooth muscle actin (a smooth muscle cell marker), and laminin alpha 2 (a base membrane protein). CFT/SPECT analysis demonstrated the accumulation of ASOs in the submandibular, deep cervical, and paraspinal lymph nodes. Wu, Su, et al. (2020) found that knockout of *AQP4* in mice reduced the brain distribution of ASOs after IT administration. The results of these studies corroborated the findings of Iliff et al. (2012), suggesting the brain distribution of 3-kDa dextran after ICM administration, indicating a role of the glymphatic system in the distribution of ASOs. However, the elimination pathway from the brain has not yet been elucidated; further studies are needed to clarify through which of the two systems—the glymphatic or IPAD systems—the administered OTs are transferred to the lymphatic system.

2.4 | Model analysis and human PK/dose prediction

The PK/PD model analysis is a powerful tool for quantitatively understanding the observed data and subsequent simulations. This enables appropriate study design for preclinical POC, rational translation of PK/PD from preclinical models to humans, mechanism-based prediction of human effective doses, and identification of optimal clinical dosing regimens. This section summarizes the application examples of modeling and simulation to CNS-targeted OTs and human PK/dose prediction methods.

Biliouris et al. (2018) developed a population PK model using NHP PK data of the approved drug nusinersen for the treatment of spinal muscular atrophy (SMA). This model consisted of compartments for the CSF, three spinal cord regions, the brain, and the pons. The model described the concentration–time profile of nusinersen in the CSF and spinal cord with reasonably high accuracy, but not in the brain. The volumes of distribution in the CSF and spinal cord compartments were comparable to physiological volumes of CSF and the spinal cord, respectively. The study also examined body weight-based allometric scaling-up in pediatric patients from NHP data. Such allometric scaling-up generally described clinical CSF drug concentrations by applying age-based CSF volumes (120 ml for <0.25 years, 130 ml for <0.25–0.5 years, 140 ml for 1–2 years, 150 ml for >2 years), as well as allometry exponent values of −0.08 for the rate constant and 1 for tissue distribution volume.

For tominersen targeting *HTT*, a simpler brain compartment model with first-order absorption and elimination was constructed (Tabrizi et al., 2019). A PK/PD model was created assuming that humanized transgenic mice are a good predictor of effective human concentration. Human PK prediction was performed based on a PK model for NHPs. The developed PK/PD model reflected the actual data in mice and NHPs. When the PK scaling took into account species differences in CSF volume for distribution volume, *HTT* protein levels in human CSF were predicted with reasonable accuracy.

Such a simple normalization on the PK scaling by CSF volume was suggested to be highly useful for PK/PD/dose prediction after IT administration. The usefulness of this method has been demonstrated to some extent in preclinical studies. When the dose was normalized by the CSF volume, generally consistent ASO concentrations in the spinal cord near the IT injection site were obtained between rat and NHPs (Jafar-Nejad et al., 2021). In contrast, ASO concentrations in mouse and rat brains, distal to the injection site, were lower than those in NHPs at similar dose levels normalized by CSF volume. As described in Section 2.2, tissue concentration might be affected by multiple factors, ROA, and dose volume. Therefore, the prediction of brain concentration based on CSF volume normalization should be carefully handled. This CSF volume normalization method would depend on the dosing condition and may not always be applicable.

A physiologically-based pharmacokinetic (PBPK) model has also been reported to incorporate more physiological factors, such as tissue volume and CSF volume (Monine et al., 2021). Data collected over 6 months in a study of repeated IT dosing of 2′-MOE gapmer ASOs (4–35 mg) to NHPs were subjected to modeling using the physiological tissue volume and the CSF volume. The constructed model well described the observed concentration data in several brain regions, the spinal cord, CSF, plasma, liver, and kidney. However, in this model the transition process between CSF of each compartment (e.g. CSF at the cervical cord to CSF in the proximal brain) was not connected by CSF bulk flow but was characterized by simple rate constant parameters. This might be due to the unique situation of IT administration. After IT administration, ASO is distributed against CSF bulk flow, especially from the ventricles to the cisterna magna. Additionally, because of the slow velocity of CSF bulk flow, their distribution can be influenced by the external convective force and gravity associated with body position (Sullivan et al., 2020). Moreover, the injection volume and speed have a significant impact on CSF distribution and subsequent mRNA knockdown (Wolf et al., 2016). Unlike rapid diffusion from arterial blood to tissue microvessel blood after intravenous (IV) administration, fluid dynamics, including the concentration gradient and pulsation, require consideration for the mechanistic modeling of brain distribution after IT/ICV administration (Aldea et al., 2019; Hsu et al., 2012). The PK/PD projection, incorporating the spatial distribution of OTs to each brain region via CSF flow, has not been performed. A fully physiological and mechanistic CSF spatial

distribution model would enable the prediction of heterogeneous distribution of OTs in CSF and the brain parenchyma.

2.5 | Challenges associated with the CNS evaluation of OTs following IT and ICV administration

Various studies have been conducted on the brain distribution of ASOs after IT or ICV administration. However, further investigation on the pathway, mechanism, dose dependence, species difference, and quantitative analysis for such brain distribution is needed. These could provide valuable information to understand the impacts of differences in a compound's physicochemical properties and size on its brain distribution and subsequent human PK/dose prediction by physiologically relevant and quantitative model analysis.

3 | ALTERNATIVE ADMINISTRATION ROUTES AS A NEXT-GENERATION STRATEGY

To improve patient quality of life, a less invasive route of administration is desired for drug delivery to the brain because of the invasiveness of IT administration. This section summarizes the delivery of OTs by routes other than the IT and ICV routes.

3.1 | Nose-to-brain delivery

Directly targeting the CNS by the intranasal route is attractive from the following viewpoints: an early onset effect by rapid drug exposure in the target brain region, brain delivery of drugs that are difficult to distribute from the systemic circulation because of the presence of the BBB, and a reduction in the risk of adverse reactions by preventing unnecessary drug exposure in peripheral tissues. Additionally, since self-administration is possible, intranasal administration would be less invasive than other administration routes, including IV and IT administration. Given its attractive features, the applicability of drug delivery via the nose-to-brain route after intranasal administration has been investigated for diverse drug modalities, including OTs, peptides, proteins, cell therapies, and small-molecule compounds (Crowe & Hsu, 2022). As summarized in Figure 3, there are two pathways known for nose-to-brain drug delivery following intranasal administration; one is the route of the olfactory bulb system via absorption from the olfactory epithelium and cribriform, while the other is the route of the trigeminal nervous system following absorption from the respiratory epithelium (Wang et al., 2019).

Although information on the brain delivery of OTs by intranasal administration is limited, data from some promising studies are available. For example, Kanazawa et al. (2013, 2014, 2019) attempted to deliver siRNA to the CNS by using polyethylene glycol-polycaprolactone (PEG-PCL) polymer micelles conjugated to transactivator of transcription protein (Tat), known as a cell-penetrating peptide (CPP) (PEG-PCL-Tat). They encapsulated siRNA targeting *Raf-1* associated with cell differentiation and apoptosis with camptothecin (CPT), the small-molecule anticancer agent in PEG-PCL-Tat. They investigated the therapeutic effects of the PEG-PCL-Tat complex in a rat model of malignant glioma. At the same dosage, the brain siRNA levels were significantly higher by intranasal administration than by IV administration. Additionally, glioma regression and a significant life-prolonging effect were observed in rats treated with intranasal PEG-PCL-Tat, including anti-*Raf-1* siRNA and CPT, compared with the untreated or naked siRNA–treated group (Kanazawa et al., 2019). In a study using PEG-PCL-Tat including anti-TNF-alpha siRNA, its intranasal administration to a rat model of cerebral ischemia-reperfusion injury led to reduced TNF-alpha production, shrinkage of the infarcted area, and a significant improvement in neurological scores (Kanazawa et al., 2014). The imaging results using fluorescence-labeled PEG-PCL-Tat suggested

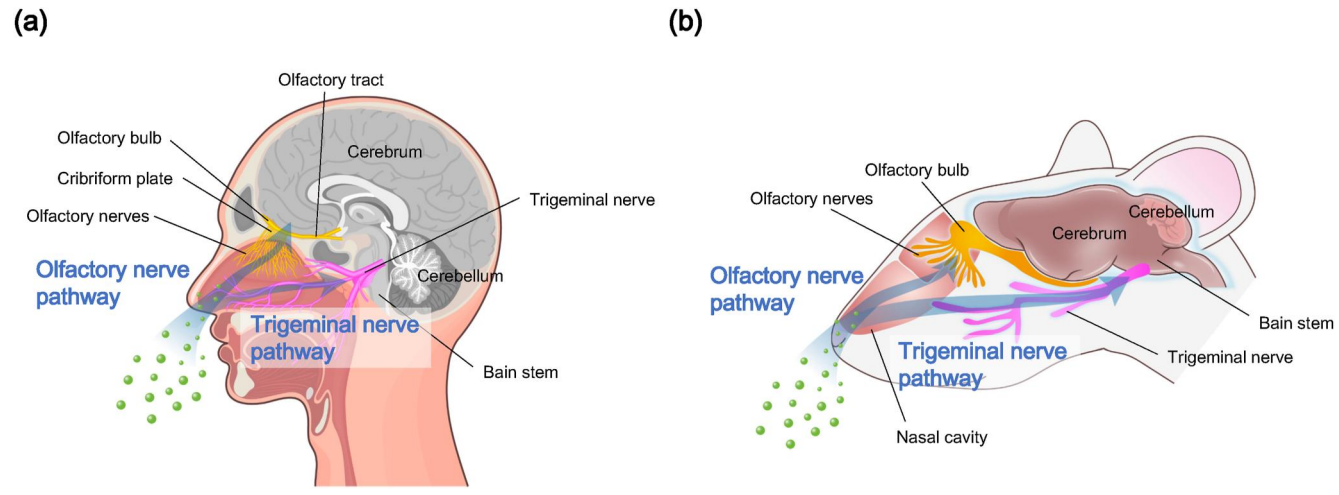

FIGURE 3 Potential pathways of direct nose-to-brain delivery of therapeutics in (a) humans and (b) rodents. Two major pathways are known for nose-to-brain drug delivery; one is the olfactory nerve pathway via absorption from the olfactory epithelium and cribriform, and the other is the trigeminal nerve pathway following absorption from the respiratory epithelium

that both the routes via the olfactory bulb and the trigeminal nerve could be involved in the nose-to-brain delivery of PEG-PCL-Tat (Kanazawa et al., 2013).

Similarly, studies using nanoparticle (NP) formulations have been reported; siRNA delivery to the CNS using chitosan NPs has been investigated intensively. Chitosan forms NPs through polymerization by electrostatic interactions between the positive charge of its amino group and the negative charge of the phosphate group of siRNA (Sanchez-Ramos et al., 2018). In a study using chitosan-based NPs loaded with anti-HTT siRNA, intranasal administration reduced HTT mRNA levels by at least 50% in the olfactory bulb, hippocampus, corpus striatum, and cerebral cortex of YAC128 mice, which is a model of Huntington's disease (Sava et al., 2020).

In a study where hyaluronic acid (HA)/DP7-C nanomicelles—formed by the self-assembly of DP7-C (CPP comprising 12 amino acids) followed by a coating of its surface with HA—were used as a carrier, the therapeutic effects of siRNA targeting *VEGF* and *PLK1* (targets in glioblastoma treatment), were assessed by the intranasal route. In GL261 tumor-bearing mice, once-daily intranasal administration of HA/DP7-C/siVEGF or HA/DP7-C/siPLK1 reduced target protein levels, suppressed angiogenesis, regressed brain tumor, and prolonged survival. Bioimaging of the distribution of siRNA administered by the intranasal route revealed no signal in the olfactory bulb. However, it showed its transfer to the pons via the trigeminal nerve, followed by distribution throughout the brain. HA coating is expected to increase the viscosity of the nanomicelles, leading to an increase in their residence time in the nasal cavity. It is also suggested to enable more effective delivery of the nanomicelles to the target cancer cells via CD44, which is a receptor of HA and is highly expressed on the surface of cancer cells, thus mediating the delivery of HA-coated nanomicelles by the CD44–HA interaction (Yang et al., 2022).

Several studies have been published on the target cell-specific brain delivery of siRNA or ASOs conjugated to a small-molecule inhibitor using intranasal administration. Bortolozzi et al. (2021) conjugated OTs to monoamine transporter (MAT) inhibitors, such as sertraline, reboxetine, and indatraline, and successfully delivered the nucleic acids to the targeted brainstem monoamine neurons by intranasal administration. When the anti-5-HT_{1A} receptor siRNA was conjugated to sertraline, a selective serotonin reuptake inhibitor, and administered to wildtype mice by the intranasal route, the conjugated siRNA induced knockdown of the 5-HT_{1A} receptor and elicited an antidepression-like response to an extent similar to that by ICV administration of the same dose (Bortolozzi et al., 2012). In a study using siRNA targeting the serotonin transporter (SERT), its 7-day administration reduced SERT mRNA levels by 50% in the mouse dorsal raphe nucleus (DR) (Ferres-Coy et al., 2016). When anti-alpha-synuclein ASOs or siRNA were conjugated to indatraline and administered to normal mice once daily for 4 days at 30-μg/day, alpha-synuclein mRNA levels were significantly reduced by ~30% (Alarcon-Aris et al., 2018). In a study using siRNA targeting TASK3, the use of sertraline or reboxetine as a ligand successfully reduced TASK3 mRNA and protein levels in the target neurons, serotonin (5-HT) neurons for sertraline, and norepinephrine neurons for sertraline in the brain stem (Fullana et al., 2019). Although details of the drug transport mechanism for the brain distribution of intranasal oligos conjugated to a MAT inhibitor are not fully understood, the transport of the extracellular pathway via CSF by pulsatile flow and subsequent uptake by the dense network of axons are discussed as a possible mechanism (Alarcon-Aris et al., 2018). Notably, in these intranasal administration studies of oligos conjugated to an MAT inhibitor, phosphate-buffered saline (PBS)-based dosing solutions were used, and effective brain neuron targeting was achieved without devising special pharmaceutical techniques.

The role of microRNA in CNS targeting of OTs by intranasal administration has also been investigated. Ma et al. (2016) administered complementary LNA oligonucleotides targeting microRNA-210 (miR-210-LNA) to a rat model of hypoxic-ischemic brain injury by the intranasal route; they found that miR-210-LNA significantly downregulated brain miR-210 levels and dose-dependently reduced the brain infarct size. Similarly, intranasal administration of LNA-modified antagomir targeting miRNA-134 significantly reduced miRNA-134 levels in the mouse brain (Jimenez-Mateos et al., 2012).

In a mouse model of spared nerve injury, intranasal administration of anti-HuR ASOs (18-mer) mixed with 1,2-dioleoyl-3-trimethylammonium-propane, an artificial cationic lipid, significantly reduced HuR protein in the spinal cord and improved allodynia to the extent that IT administration did (Borgonetti & Galeotti, 2021). In a rat intracerebral tumor xenograft model, intranasal administration of the 13-mer oligonucleotide GRN163, developed as a telomerase inhibitor, resulted in its tumor-specific distribution, tumor regression, and a significant improvement in survival rate (Hashizume et al., 2008).

3.2 | Brain delivery via systemic administration

CNS targeting of OTs has been intensively investigated by systemic administration and intranasal administration. Just as intranasal administration was discussed above, in this section, we expand the focus on systemic administration. There are high expectations for the establishment of delivery techniques by systemic administration of OTs for the following reasons. (1) Systemic administration is less invasive than IT administration, leading to an improvement in patient QOL; (2) it requires no advanced techniques or special administration device; and (3) it may enable homogeneous distribution of the drug to the whole brain. This section summarizes representative nonclinical cases reported to date.

3.2.1 | Representative pathways to cross the BBB

Penetration of the BBB or blood–CSF barrier (BCSFB) is required to achieve CNS targeting of OTs by systemic administration. Several pathways are available for BBB penetration (Patel & Patel, 2017). Representative pathways are summarized in Figure 4 along with the major strategies by which OTs cross the BBB, which are discussed in detail in subsequent sections. In general, the primary pathway for

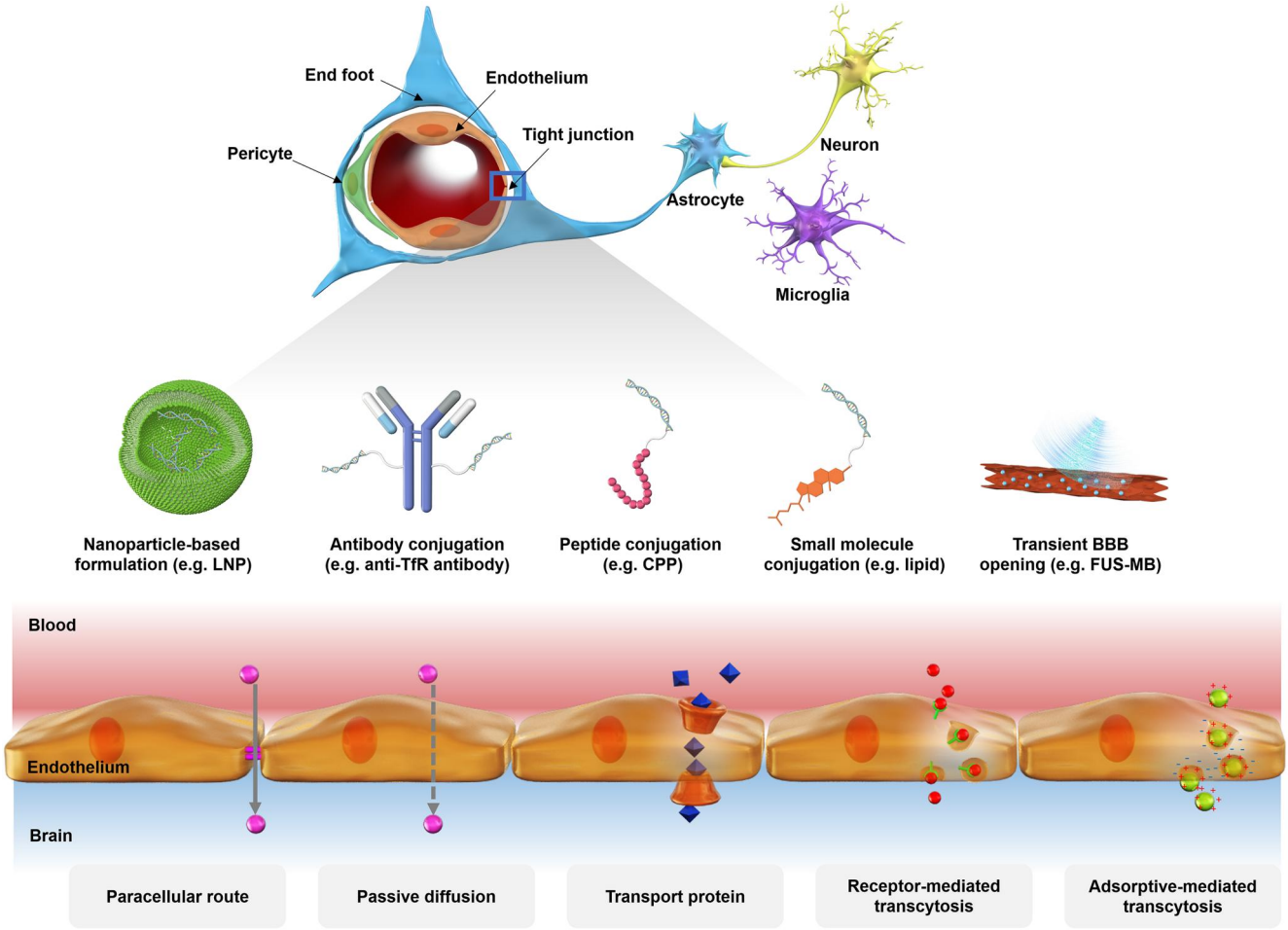

FIGURE 4 Schematic of the components of the blood–brain barrier (BBB) and its main transport pathways with the representative strategy of oligonucleotide therapeutics (OTs) crossing the BBB

penetration of the BBB by CNS drugs involves passive diffusion through endothelial cells. However, this pathway is generally limited to highly lipophilic small molecules and may not be suitable for OTs. A second pathway for specific substrates utilizes transporter proteins to mediate BBB penetration. Essential molecules, such as glucose, amino acids, monocarboxylic acids, hormones, fatty acids, carbohydrates, nucleotides, inorganic ions, amines, choline, and vitamins, can penetrate the BBB via their specific transporters (e.g. glucose-transporter 1 [GLUT1] for glucose, LAT1 for certain amino acids) (Sweeney et al., 2019). Due to the requirements of specificity and size for substrates to be moved by these transporters, it is not fully understood if OTs or their conjugates are able to utilize this pathway for crossing the BBB. The third pathway is based on endocytosis/exocytosis, subdivided into the adsorptive-mediated and receptor-mediated transcytosis pathways (AMT and RMT, respectively). The AMT pathway is triggered by electronic interactions between the negatively charged cell membrane surface and cationic molecules (e.g. CPPs composed of cationic amino acids) and allows them to penetrate the cell membrane (Herve et al., 2008). The binding of specific ligands to cell surface receptors, such as the transferrin receptor (TfR) and lipoprotein receptor-related proteins (LRPs), initiates the RMT pathway. In this pathway, drug–receptor complexes are transported across the cytoplasm via endocytic vesicles, and the drug is eventually released on the abluminal surface (Pulgar, 2018). Endocytic vesicles are formed in a clathrin- or caveolae-dependent manner, which can bypass lysosomal storage (Kimura & Harashima, 2020). Along with the abovementioned transcellular transport pathways, the paracellular transport pathway is also available for BBB penetration and utilized for delivery of OTs. The BBB strongly restricts paracellular transport by the tight (TJ) and adherens (AJ) junctions. However, some studies have shown that transient BBB opening can be achieved by the downregulation of the TJ protein claudin-5 associated with Unc5B inhibition or Basigin stimulation (Nakada-Honda et al., 2021). Additionally, transient BBB opening with focused ultrasound (FUS) has been proven tolerable in a clinical study in patients with Parkinson's disease (Gasca-Salas et al., 2021).

3.2.2 | NP-based formulations

NP formulations have most often been reported in brain-targeting strategies for OTs by systemic administration (Table 5). NP

TABLE 5 Selected examples of in vivo brain delivery of oligonucleotide therapeutics via systemic administration

Approach	Formulation/ligand	Delivery target and MOA	Nucleic acid	Target gene	Animal model	Reference
Nanoparticle-based formulation	Angiopep-2-targeted liposomes	LRP-1	siRNA	GOLPH3	U87-GFP-luciferase-bearing BALB/c mouse	Yuan et al. (2018)
	Glucose-coated polymeric nanocarriers	GLUT1	ASO	Malat1	Fasted BALB/c mouse	Min et al. (2020)
	RVG-9r-targeted lipid nanoparticles	AchR	siRNA	Ataxin3	C57 BL/6 ataxin-3 [Q69]-transgenic mouse	Conceicao et al. (2016)
	RVG-targeted exosome	AchR	siRNA	BACE1	C57BL/6 mouse	Alvarez-Erviti et al. (2011)
	T7-peptide-coated exosomes	TfR	ASO	microRNA-21	C6 glioblastoma rat	Kim et al. (2020)
Antibody conjugation	Anti-TfR antibody (OX26)	TfR	PNA	HIV-1 rev	Sprague–Dawley rat	Penichet et al. (1999)
	Anti-TfR antibody (8D3)	TfR	PMO	SMN2	SMN2 transgenic mouse (FVB.Cg-$Smn1^{tm1Hung}$ Tg(SMN2)2Hung/J)	Hammond et al. (2021)
	OTV	TfR	ASO	Malat1	Mouse	Denali-Therapeutics (2020) and Mullard (2022)
Peptide conjugation	RVG-9R	AchR	siRNA	SOD1, FvE^{J}	Balb/c mouse, JEV-infected NOD/SCID mouse	Kumar et al. (2007)
	TARBP-BTP	Monosialoganglioside GM1	siRNA	BACE1	AβPP-PS1 mouse, C57BL/6 mouse	Haroon et al. (2016, 2019)
	Pip6a	CPP	PMO	SMN2	SMN2 transgenic mouse ($Smn1^{tm1Hung/WT}$;$SMN2^{tg/tg}$)	Hammond et al. (2016)
	Branched ApoE-derived peptide	N.D.	PMO	SMN2	SMN2 transgenic mouse ($Smn1^{tm1Hung/WT}$;$SMN2^{tg/tg}$)	Shabanpoor et al. (2017)
	ApoB-derived peptide ($ApoB^{11}$)	LDL-R	siRNA	α-synuclein	α-synuclein transgenic mouse	Spencer et al. (2019)
	Melanotransferrin-derived peptide	LRP (potential target)	siRNA	NOX4	C57BL/6 mouse	Demeule et al. (2002) and Eyford et al. (2021)
Small-molecule ligand or chemical modification	Tricyclo-DNA	N.D.	ASO	SMN2	Type III SMA mouse	Robin et al. (2017)
	Cholesterol or α-tocopherol	N.D.	HDOs	Malat1, Dmpk, Gfap, SOD1	C57BL/6 mouse, Sprague–Dawley rat	Nagata et al. (2021)

TABLE 5 (Continued)

Approach	Formulation/ligand	Delivery target and MOA	Nucleic acid	Target gene	Animal model	Reference
Transient BBB opening	Definity® microbubble contrast agent and focused ultrasound	Transient BBB modulation by cavitation effects	siRNA	HTT	Wistar rat	Burgess et al. (2012)
	Bubble liposomes and high-intensity focused ultrasound	Transient BBB modulation by cavitation effects	PMO	N.A.	ICR mouse	Negishi et al. (2015)
	Angubindin-1	Tricellular tight junction opening by transient removal of angulin-1	ASO	Malat1	C57BL/6 mouse	Zeniya et al. (2018) PMID: 29753959

Abbreviations: AchR, acetylcholine receptor; ASO, antisense oligonucleotide; BACE1, beta-site APP cleaving enzyme 1; BBB, blood–brain barrier; CPP, cell-penetrating peptide; Dmpk, DM1 protein kinase; Gfap, glial fibrillary acidic protein; GLUT1, glucose-transporter 1; GOLPH3, Golgi phosphoprotein 3; HDOs, heteroduplex oligonucleotides; HIV-1, human immunodeficiency virus type 1; HTT, huntingtin; LDL-R, low-density lipoprotein receptors; LRP1, low-density lipoprotein receptor-related protein 1; Malat1, metastasis associated in lung adenocarcinoma transcript-1; MOA, mechanism of action; NOX4, NADPH oxidase 4; OTV, oligonucleotide transport vehicle; Pip6a, PMO internalizing peptide 6a; PMO, phosphorodiamidate oligomer; PNA, peptide-nucleic acid; RVG, rabies virus glycoprotein; siRNA, small interfering RNA; SMA, spinal muscular atrophy; SMN2, survival motor neuron 2; SOD1, superoxide dismutase 1; TfR, transferrin receptor.

formulations include liposomes, lipid-based NPs (LNPs), polymeric NPs, lipid–polymer hybrid NPs, modified cyclodextrins, and extracellular vesicles (Mendonca et al., 2021).

Yuan et al. (2018) showed that siRNA delivery to mouse glioma was enhanced by using angiopep-2–modified cationic liposomes, and they demonstrated a significant antiglioma effect by delivering siRNA targeting Golgi phosphoprotein 3 specifically to glioma. Angiopep-2 is a 19-amino-acid specific substrate for low-density lipoprotein receptor-related protein 1 (LRP-1), a member of the low-density lipoprotein receptor (LDL-R) family known to be related to RMT (Demeule et al., 2008). In an assessment using siRNA fluorescently labeled with Cy5, angiopep-2–modified cationic liposomes increased siRNA delivery to the brain ~3-fold compared with naked siRNA. Using a novel liposome (DCL64) comprising dipalmitoylphosphatidylcholine, cholesterol, and poloxamer L64, Ashizawa et al. (2019) successfully delivered single-stranded oligonucleotides to the mouse cerebellar Purkinje cells through interactions between DCL64 and the LDL-R.

Min et al. (2020) demonstrated the BBB crossing of ASOs via GLUT1 in mice using glucose-coated polyion complex micelles. The designed nanocarriers encapsulating *Malat1*-targeting ASOs were effectively distributed to a wide range of brain regions, including the cerebrum and hippocampus, after IV administration. Additionally, IV administration of 100 μg of ASOs showed a knockdown efficiency of >50% at 24 h postdose. Interestingly, there is a bell-shaped curve relationship between the number of glucose molecules modifying each NP and the amount of ASOs transferred to the brain or the intensity of their knockdown effect; ~50 glucose molecules per particle 50 nm in diameter yielded the highest delivery efficiency. All these results suggest that controlling ligand density on the NP surface or optimizing the binding–dissociation balance based on multivalent interactions between the ligand and receptor is essential for effective delivery through RMT-based BBB crossing.

Several studies have investigated the use of a short peptide derived from rabies virus glycoprotein (RVG), a ligand of the nicotinic acetylcholine receptor, as a delivery ligand. Alvarez-Erviti et al. (2011) investigated siRNA delivery to the CNS using murine self-derived dendritic exosomes modified with a neuron-specific RVG peptide. In mice, IV-injected siRNA was explicitly delivered to neurons, microglia, and oligodendrocytes in the brain, resulting in the strong mRNA (60%) and protein (62%) knockdown of beta-site APP cleaving enzyme 1 (BACE1), a pharmacological target in the treatment of Alzheimer's disease. Conceicao et al. (2016) attempted CNS delivery of siRNA targeting ataxin-3 using a cationic LNP comprising 1,2-dioleoyl-3-dimethylammonium-propane, cholesterol, and 1,2-distearoyl-*sn*-glycero-3-phosphocholine and modified with an RVG-9r peptide. In a C57BL/6 *ataxin-3* [Q69] transgenic mouse model, IV administration of 2.5 mg/kg of siRNA for 3 days resulted in significant decreases in mutant ataxin-3 mRNA and aggregated protein. Additionally, the authors successfully induced reductions in neuropathology and motor behavior deficits in two mouse models of Machado–Joseph disease.

In a study investigating TfR as a delivery target, Kim et al. (2020) assessed the distribution of exosomes (T7-exo), the surface of which was decorated with the TfR-binding peptide T7, to the brain in an

intracranial glioblastoma rat model. IV administration of T7-exo–encapsulated Cy5-labeled ASOs targeting miR-21 was associated with their evident brain distribution, miRNA-21 knockdown by ~80%, and tumor regression.

3.2.3 | Antibody-conjugated oligonucleotides

Studies involving brain delivery via RMT elucidate strategies for directly conjugating nucleic acids to antibodies. In rats, Penichet et al., 1999 examined the brain distribution of HIV-1 rev–targeting antisense peptide-nucleic acid (PNA) that was conjugated to OX26, an antirat TfR antibody, through avidin–biotin interactions. The permeability-surface area (PS) product and the brain uptake were 5.6-fold and 14.5-fold, respectively, higher for the conjugated PNA than for naked PNA (Penichet et al., 1999). Hammond et al. (2021) revealed that conjugation of phosphorodiamidate oligomers (PMOs) targeting survival motor neuron 2 (SMN2) to $8D3_{130}$, an antimouse TfR antibody, was associated with effective delivery of the PMOs to the brain and spinal cord, as well as splice modulation of *SMN2*. Interestingly, the presence of an optimal binding affinity for the crossing of the BBB of an antitransferrin receptor antibody has been reported (Webster et al., 2017). These studies used an antibody with an increased K_D value, which was obtained by amino acid substitution. Denali Therapeutics (South San Francisco, CA, USA), partnering with Secarna Pharmaceuticals (Planegg, Germany), is also developing a portfolio aiming at the BBB crossing and CNS delivery of nucleic acids by using a unique delivery platform (oligonucleotide transport vehicle) with a low-affinity TfR-binding site in the Fc domain of the antibody. Although no detailed information has been published on the target genes of the candidate product for clinical development, knockdown of *Malat1* mRNA by 50% has been reported in the mouse cortex and spinal cord (Mullard, 2022).

3.2.4 | Peptide ligand conjugation

The CNS delivery of OTs conjugated to a peptide as a smaller delivery ligand has also been investigated actively.

Using siRNA conjugated to a 41-amino-acid peptide (RVG-9R) targeting the acetylcholine receptor, Kumar et al. (2007) successfully increased the brain uptake of siRNA and significantly decreased mRNA levels of the target gene without affecting the distribution of the siRNA to the spleen or liver. Additionally, 4-day IV administration of the antiviral FvE^J siRNA–RVG-9R complex (50 μg of siRNA per mouse) improved survival to 80% in JEV-induced encephalitis mice.

Haroon et al. (2016) investigated the delivery of siRNA to the mouse brain using the fusion protein TARBP-BTP, comprising a double-stranded RNA-binding domain of the human transactivation response element (TAR) RNA-binding protein (TARBP2) fused to a brain-targeting peptide that binds to monosialoganglioside GM1. The use of this platform resulted in the brain distribution of siRNA targeting BACE1, a significantly potent mRNA knockdown effect compared with that by naked siRNA, accompanied by improvements in spatial learning and memory in an Alzheimer's disease model (AβPP-PS1 mice).

In addition to the delivery mechanism targeting the cell surface receptor, research has also been conducted on targeting the CNS using CPPs. Hammond et al. (2016) investigated the delivery of PMOs to peripheral and CNS tissues using arginine-rich CPPs. A PMO-internalizing peptide (Pip6a) comprising a 22-amino-acid was conjugated to a PMO sequence targeting the ISS-N1 element of *SMN2* intron 7 and administered IV to human *SMN2* transgenic mice twice at 18 mg/kg to assess its skipping effect. A significant increase in full-length *SMN2* expression was detected in the cortex, brain stem, and cerebellum. Shabanpoor et al. (2017) found that a branched derivative of the ApoE (141–150) peptide effectively delivered PMOs to the CNS. Its conjugation to PMOs targeting *SMN2* exon 7 inclusion resulted in a significant increase in the *SMN2* pre-mRNA exon inclusion level in the CNS and peripheral tissues of an SMA mouse model, as well as pharmacological effects, including prolonged average lifespan in the model. Although the ApoE (141–150) derivative peptide is also an arginine-rich peptide, it remains unknown whether the mechanism for its CNS delivery is attributed to AMT or RMT; for example, by the ApoE receptor, or some combination of the two.

Spencer et al. (2019) conjugated an 11-amino-acid sequence from the apolipoprotein B protein to siRNA targeting α-synuclein (α-syn) using a 9-amino-acid arginine linker to investigate whether the nucleic acids can be delivered to neuronal and glial cells through LDL-R–mediated BBB crossing. When the siRNA (50 μg/head) was administered intraperitoneally to *α-syn* transgenic mice twice weekly for 4 weeks, the α-syn protein level was reduced by >50% in the neocortex, hippocampus, and striatum. In a study by Eyford et al. (2021), a 12-amino-acid peptide derived from melanotransferrin, which has been suggested to involve transcytosis through interactions with LRPs, was used as a delivery ligand; they reported the delivery of NOX4-targeting siRNA to brain parenchymal cells and decreased Nox4 mRNA and infarct volume in a mouse model of ischemic stroke.

3.2.5 | Chemical modification and small-molecule ligands

Robin et al. (2017) examined the CNS transfer of tricyclo-DNA ASOs, a class of conformationally constrained DNA analogs. When ASOs (200 mg/kg) targeting exon 7 inclusion in SMN2 mRNA were administered subcutaneously to type-III SMA mice once weekly for 12 weeks, a significant increase in exon inclusion was detected in the brain in addition to peripheral muscle tissue (Robin et al., 2017).

Recently, Nagata et al. (2021) found that DNA/RNA heteroduplex oligonucleotides (HDOs) conjugated to lipids as a delivery ligand had a high potential for CNS distribution and a potent mRNA

knockdown effect. In mice and rats, HDOs conjugated to cholesterol or α-tocopherol at the 5′ end of the RNA strand were distributed throughout the brain and transferred to the spinal cord after subcutaneous (SC) or IV administration. Additionally, the HDOs exhibited dose-dependent PK/PD on the four target genes, including *Malat1*; once-daily administration at 50 mg/kg for 4 weeks achieved 90% gene knockdown. In contrast, single-stranded ASOs conjugated to cholesterol produced only a limited knockdown effect, showing that conjugated HDOs are essential for effective CNS delivery. Moreover, adverse reactions such as thrombocytopenia and focal brain necrosis were successfully reduced by using SC delivery or dividing IV injections, while the knockdown effects were maintained. Although direct comparison is impossible, no other studies have shown that systemic administration of ASOs achieved as high as 90% gene knockdown without direct BBB opening.

3.2.6 | Transient BBB opening

An investigation has been conducted on the delivery of nucleic acids to the CNS by the paracellular route through transient loosening of the BBB tight junctions. Zeniya et al. (2018) focused on angubindin-1, a novel binder to angulin-1 and angulin-3, which are components of the tricellular TJ, and assessed the effect of the novel binder in delivering ASOs to the CNS. IV administration of angubindin-1 followed by that of *Malat1*-targeting ASOs 1 h later resulted in a brain ASO level markedly higher than that of ASOs alone. Additionally, *Malat1* RNA levels decreased depending on the ASO dose, with ~40% knockdown. The in vitro BBB model study and in vivo imaging suggested that the BBB opening induced by angubinidin-1 administration was reversible and transient. No noticeable adverse reactions attributable to angubinidin-1 were observed in mice.

Investigations have also been conducted on the CNS delivery of nucleic acids through transient BBB modulation based on a cavitation effect by combining microbubble administration and ultrasound irradiation. Negishi et al. (2015) examined whether the method for transiently enhancing BBB permeability by combining echo-contrast gas (C_3F_8) entrapping liposomes (bubble liposomes) and high-intensity FUS can be applied to the CNS delivery of nucleic acids. Fluorescent-labeled PMOs and bubble liposomes were administered IV to mice. FUS was also exposed to the right hemisphere of the mice at 1.5 kW/cm^2 for 30 s. Fluorescent signals specific to the irradiation site were detected. Similarly, Burgess et al. (2012) administered a microbubble contrast agent combined with cholesterol-conjugated siRNA targeting *HTT* mRNA IV to rats and then exposed FUS locally to the striatum of the rats. *HTT* knockdown occurred depending on the dose of nucleic acids in the striatum. Combining microbubbles and FUS in enhancing BBB permeability was shown to return to baseline within 6–24 h following FUS exposure (O'Reilly et al., 2017). There have been some clinical studies on such combination effects (Wu, Tsai, et al., 2020), including the delivery of chemotherapy combined with FUS to the brain of the glioma patients (Mainprize et al., 2019).

3.2.7 | Model analysis after systemic administration

Recently, Goto et al. (2022) reported the PK/PD analysis of systemically administered cholesterol-conjugated HDOs (Chol-HDO). A model was constructed based on the PK/PD data on Chol-HDOs, which enabled the delivery of ASOs into the whole brain after IV administration. This analysis suggested the presence of a rate-limiting step during the distribution process to target cell nuclei; thus, an effective site (deep) compartment was included to describe the saturation process and delay of the knockdown effect from an apparent ASO concentration increase in brain. Interestingly, similar deep compartment (effective site compartment) has often been incorporated for the target tissue in analyses of other systemically administered ASOs and siRNAs (Mukashyaka et al., 2021). Possible explanations of a delay of knockdown effect modeled by deep brain compartment include the presence of storage and slow release from deposits at the cell level (macrophages and endothelial cells) and organelle level (endosomes/lysosomes) (Crooke et al., 2017; Linnane et al., 2019; Nagata et al., 2021).

Recently, improvements in targeting and subsequent pharmacological activity by using various DDSs and chemical modifications have been reported, as described in Sections 3.2.1–3.2.6. Translation on each of the following steps is required for rational PK/PD/dose prediction of the OT DDS after systemic administration: (1) systemic kinetics, (2) BBB penetration, and (3) intrabrain and intracellular distribution and elimination. Allometry is commonly used to scale up systemic ASO kinetics (Di Martino et al., 2019; Geary, 2009). For scaling up on BBB and BCSFB penetration, consideration of species differences in the penetration mechanism and its rate is necessary. Additionally, scaling-up on intrabrain distribution and elimination requires consideration of physiological and anatomical species differences involving the distribution and elimination pathways described in Section 2.2. Quantitative and translational analysis on CNS targeting OTs after systemic dosing has been limited, and thus, further advances in this field are anticipated.

3.3 | Challenges associated with alternative OT administration routes to the brain

As described above, platform studies aimed to deliver OTs to the CNS by intranasal or systemic administration as a noninvasive alternative to IT administration have been conducted actively; these methods are expected to be put into practical use. Nevertheless, the studies currently available are still limited to POC studies in rodents; therefore, advances in POC studies in nonrodents considering clinical application are eagerly awaited. For intranasal administration, target species with nasal cavity and brain structures closer to humans (e.g. NHPs) are essential. Additionally, due to the limitation of applicable dosing volume (~100 μl per nostril in adult human) (Marx et al., 2015), drug product optimization and administration device development for clinical application are critical. For systemic administration, the ratio of drug exposure in peripheral organs to

that in the brain tends to be higher than for IT administration; therefore, OTs designed with higher activity and safety would be required to ensure a sufficiently high therapeutic index. Notably, dysfunction of the BBB has been reported in several CNS pathological conditions, including multiple sclerosis, hypoxic and ischemic insult, Parkinson's disease, Alzheimer's disease, lysosomal storage disease, and brain tumors (Kadry et al., 2020). The change in BBB integrity needs to be considered for data interpretation in the preclinical disease models as well as for the translation of CNS targeting effect from preclinical models toward patients. In addition to crossing the BBB, there are a couple of other potential routes to access the CNS. Some of them are from the systemic blood circulation, including the bypass via BCSFB, blood–arachnoid barrier, blood–spinal cord barrier (Uchida et al., 2022), and even the delivery from the neuromuscular junction to the anterior horn cells of the spinal cord by retrograde axonal transport (Ovsepian et al., 2015). Investigation of these additional routes should be of value to realize the delivery of OTs for CNS via systemic administration.

4 | CONCLUSIONS AND FUTURE PERSPECTIVES

This review summarizes brain distribution profiles and pathways of OTs after IT/ICV administration and alternative administration routes. Although many studies to date have provided information, much remains to be clarified, described in the following three points. (1) Elucidating details of the pathways and molecular mechanisms for the brain distribution of OTs will lead to a better understanding of their regional and cellular distribution and, ultimately, of species differences in their brain delivery; understanding of the concentration-dependence on its mechanism will allow the interpretation of the dose-dependence. (2) Physiological and anatomical species differences in the brain are critical factors. Differences in brain tissue morphology and size, CSF flow pathway/rate, CSF volume, and BBB/BCSFB area and tightness can also influence brain OT distribution. (3) Finally, quantitative interpretation of intracellular OT distribution, including uptake by target cells, endosomal escape, and transition to the target cell nucleus, is critical for predicting drug efficacy. Further research on these topics for OTs is essential for appropriate translation to humans and contributes to improving human PK/dose prediction, warranting further accumulation of knowledge on such areas.

ACKNOWLEDGMENT

No acknowledgments.

CONFLICT OF INTEREST

All authors are employees of Takeda Pharmaceutical Company Limited.

DATA AVAILABILITY STATEMENT

Data sharing is not applicable to this article, as no new data were created or analyzed in this study.

ORCID

Akihiko Goto https://orcid.org/0000-0001-6294-4961
Shinji Iwasaki https://orcid.org/0000-0001-5339-8372

REFERENCES

Ait Benichou, S., Jauvin, D., De Serres-Berard, T., Pierre, M., Ling, K. K., Bennett, C. F., Rigo, F., Gourdon, G., Chahine, M., & Puymirat, J. (2022). Antisense oligonucleotides as a potential treatment for brain deficits observed in myotonic dystrophy type 1. *Gene Therapy*. https://doi.org/10.1038/s41434-022-00316-7

Alarcon-Aris, D., Recasens, A., Galofre, M., Carballo-Carbajal, I., Zacchi, N., Ruiz-Bronchal, E., Pavia-Collado, R., Chica, R., Ferres-Coy, A., Santos, M., Revilla, R., Montefeltro, A., Farinas, I., Artigas, F., Vila, M., & Bortolozzi, A. (2018). Selective alpha-synuclein knockdown in monoamine neurons by intranasal oligonucleotide delivery: Potential therapy for Parkinson's disease. *Molecular Therapy*, *26*(2), 550–567. https://doi.org/10.1016/j.ymthe.2017.11.015

Aldea, R., Weller, R. O., Wilcock, D. M., Carare, R. O., & Richardson, G. (2019). Cerebrovascular smooth muscle cells as the drivers of intramural periarterial drainage of the brain. *Frontiers in Aging Neuroscience*, *11*, 1. https://doi.org/10.3389/fnagi.2019.00001

Alterman, J. F., Godinho, B., Hassler, M. R., Ferguson, C. M., Echeverria, D., Sapp, E., Haraszti, R. A., Coles, A. H., Conroy, F., Miller, R., Roux, L., Yan, P., Knox, E. G., Turanov, A. A., King, R. M., Gernoux, G., Mueller, C., Gray-Edwards, H. L., Moser, R. P., … Khvorova, A. (2019). A divalent siRNA chemical scaffold for potent and sustained modulation of gene expression throughout the central nervous system. *Nature Biotechnology*, *37*(8), 884–894. https://doi.org/10.1038/s41587-019-0205-0

Alvarez-Erviti, L., Seow, Y., Yin, H., Betts, C., Lakhal, S., & Wood, M. J. (2011). Delivery of siRNA to the mouse brain by systemic injection of targeted exosomes. *Nature Biotechnology*, *29*(4), 341–345. https://doi.org/10.1038/nbt.1807

Ashizawa, A. T., Holt, J., Faust, K., Liu, W., Tiwari, A., Zhang, N., & Ashizawa, T. (2019). Intravenously administered novel liposomes, DCL64, deliver oligonucleotides to cerebellar Purkinje cells. *The Cerebellum*, *18*(1), 99–108. https://doi.org/10.1007/s12311-018-0961-2

Aspelund, A., Antila, S., Proulx, S. T., Karlsen, T. V., Karaman, S., Detmar, M., Wiig, H., & Alitalo, K. (2015). A dural lymphatic vascular system that drains brain interstitial fluid and macromolecules. *Journal of Experimental Medicine*, *212*(7), 991–999. https://doi.org/10.1084/jem.20142290

Biliouris, K., Gaitonde, P., Yin, W., Norris, D. A., Wang, Y., Henry, S., Fey, R., Nestorov, I., Schmidt, S., Rogge, M., Lesko, L. J., & Trame, M. N. (2018). A semi-mechanistic population pharmacokinetic model of nusinersen: An antisense oligonucleotide for the treatment of spinal muscular atrophy. *CPT: Pharmacometrics & Systems Pharmacology*, *7*(9), 581–592. https://doi.org/10.1002/psp4.12323

Borgonetti, V., & Galeotti, N. (2021). Intranasal delivery of an antisense oligonucleotide to the RNA-binding protein HuR relieves nerve injury-induced neuropathic pain. *Pain*, *162*(5), 1500–1510. https://doi.org/10.1097/j.pain.0000000000002154

Bortolozzi, A., Castane, A., Semakova, J., Santana, N., Alvarado, G., Cortes, R., Ferres-Coy, A., Fernandez, G., Carmona, M. C., Toth, M., Perales, J. C., Montefeltro, A., & Artigas, F. (2012). Selective siRNA-mediated suppression of 5-HT1A autoreceptors evokes strong anti-depressant-like effects. *Molecular Psychiatry*, *17*(6), 612–623. https://doi.org/10.1038/mp.2011.92

Bortolozzi, A., Manashirov, S., Chen, A., & Artigas, F. (2021). Oligonucleotides as therapeutic tools for brain disorders: Focus on major depressive disorder and Parkinson's disease. *Pharmacology & Therapeutics*, *227*, 107873. https://doi.org/10.1016/j.pharmthera.2021.107873

Brown, K. M., Nair, J. K., Janas, M. M., Anglero-Rodriguez, Y. I., Dang, L. T. H., Peng, H., Theile, C. S., Castellanos-Rizaldos, E., Brown, C., Foster,

D., Kurz, J., Allen, J., Maganti, R., Li, J., Matsuda, S., Stricos, M., Chickering, T., Jung, M., Wassarman, K., … Jadhav, V. (2022). Expanding RNAi therapeutics to extrahepatic tissues with lipophilic conjugates. *Nature Biotechnology*, *40*(10), 1500–1508. https://doi.org/10.1038/s41587-022-01334-x

Burgess, A., Huang, Y., Querbes, W., Sah, D. W., & Hynynen, K. (2012). Focused ultrasound for targeted delivery of siRNA and efficient knockdown of Htt expression. *Journal of Controlled Release*, *163*(2), 125–129. https://doi.org/10.1016/j.jconrel.2012.08.012

Carare, R. O., Bernardes-Silva, M., Newman, T. A., Page, A. M., Nicoll, J. A., Perry, V. H., & Weller, R. O. (2008). Solutes, but not cells, drain from the brain parenchyma along basement membranes of capillaries and arteries: Significance for cerebral amyloid angiopathy and neuroimmunology. *Neuropathology and Applied Neurobiology*, *34*(2), 131–144. https://doi.org/10.1111/j.1365-2990.2007.00926.x

Carare, R. O., Hawkes, C. A., & Weller, R. O. (2014). Afferent and efferent immunological pathways of the brain. Anatomy, function and failure. *Brain, Behavior, and Immunity*, *36*, 9–14. https://doi.org/10.1016/j.bbi.2013.10.012

Chan, K. K., Liu, Z., Xie, Z., Chiu, M., Wang, H., Chen, P., Dunkerson, S., Liu, S., Triantafillou, G., Garzon, R., Croce, C. M., Byrd, J. C., Muthusamy, N., & Marcucci, G. (2010). A novel ultrasensitive hybridization-based ELISA method for 2-methoxyphosphorothiolate microRNAs and its in vitro and in vivo application. *The AAPS Journal*, *12*(4), 556–568. https://doi.org/10.1208/s12248-010-9214-0

Cheng, A., Li, M., Liang, Y., Wang, Y., Wong, L., Chen, C., Vlassov, A. V., & Magdaleno, S. (2009). Stem-loop RT-PCR quantification of siRNAs in vitro and in vivo. *Oligonucleotides*, *19*(2), 203–208. https://doi.org/10.1089/oli.2008.0176

Chong, S., Agarwal, S., Agarwal, S., Aluri, K. C., Arciprete, M., Brown, C., Charisse, K., Cichocki, J., Fitzgerald, K., Goel, V., Gu, Y., Guenther, D., Habtemariam, B., Jadhav, V., Janas, M., Jayaraman, M., & Castellanos-Rizaldos, E. (2021). The nonclinical disposition and PK/PD properties of GalNAc-conjugated siRNA are highly predictable and build confidence in translation to man. *Drug Metabolism and Disposition: The Biological Fate of Chemicals*, *50*(6), 781–797. https://doi.org/10.1124/dmd.121.000428

Conceicao, M., Mendonca, L., Nobrega, C., Gomes, C., Costa, P., Hirai, H., Moreira, J. N., Lima, M. C., Manjunath, N., & Pereira de Almeida, L. (2016). Intravenous administration of brain-targeted stable nucleic acid lipid particles alleviates Machado-Joseph disease neurological phenotype. *Biomaterials*, *82*, 124–137. https://doi.org/10.1016/j.biomaterials.2015.12.021

Crooke, S. T., Liang, X. H., Baker, B. F., & Crooke, R. M. (2021). Antisense technology: A review. *Journal of Biological Chemistry*, *296*, 100416. https://doi.org/10.1016/j.jbc.2021.100416

Crooke, S. T., Wang, S., Vickers, T. A., Shen, W., & Liang, X. H. (2017). Cellular uptake and trafficking of antisense oligonucleotides. *Nature Biotechnology*, *35*(3), 230–237. https://doi.org/10.1038/nbt.3779

Crowe, T. P., & Hsu, W. H. (2022). Evaluation of recent intranasal drug delivery systems to the central nervous system. *Pharmaceutics*, *14*(3), 629. https://doi.org/10.3390/pharmaceutics14030629

Demeule, M., Currie, J. C., Bertrand, Y., Che, C., Nguyen, T., Regina, A., Gabathuler, R., Castaigne, J. P., & Beliveau, R. (2008). Involvement of the low-density lipoprotein receptor-related protein in the transcytosis of the brain delivery vector angiopep-2. *Journal of Neurochemistry*, *106*(4), 1534–1544. https://doi.org/10.1111/j.1471-4159.2008.05492.x

Demeule, M., Poirier, J., Jodoin, J., Bertrand, Y., Desrosiers, R. R., Dagenais, C., Nguyen, T., Lanthier, J., Gabathuler, R., Kennard, M., Jefferies, W. A., Karkan, D., Tsai, S., Fenart, L., Cecchelli, R., & Beliveau, R. (2002). High transcytosis of melanotransferrin (P97) across the blood-brain barrier. *Journal of Neurochemistry*, *83*(4), 924–933. https://doi.org/10.1046/j.1471-4159.2002.01201.x

Denali-Therapeutics. (2020). Transporting biotherapeutics across the blood-brain barrier. https://www.denalitherapeutics.com/sites/default/files/2021-02/Denali%20BBB%20Webinar_10152020.pdf

DeVos, S. L., Miller, R. L., Schoch, K. M., Holmes, B. B., Kebodeaux, C. S., Wegener, A. J., Chen, G., Shen, T., Tran, H., Nichols, B., Zanardi, T. A., Kordasiewicz, H. B., Swayze, E. E., Bennett, C. F., Diamond, M. I., & Miller, T. M. (2017). Tau reduction prevents neuronal loss and reverses pathological tau deposition and seeding in mice with tauopathy. *Science Translational Medicine*, *9*(374). https://doi.org/10.1126/scitranslmed.aag0481

Diem, A. K., MacGregor Sharp, M., Gatherer, M., Bressloff, N. W., Carare, R. O., & Richardson, G. (2017). Arterial pulsations cannot drive intramural periarterial drainage: Significance for Aβ drainage. *Frontiers in Neuroscience*, *11*, 475. https://doi.org/10.3389/fnins.2017.00475

Di Martino, M. T., Arbitrio, M., Fonsi, M., Erratico, C. A., Scionti, F., Caracciolo, D., Tagliaferri, P., & Tassone, P. (2019). Allometric scaling approaches for predicting human pharmacokinetic of a locked nucleic acid oligonucleotide targeting cancer-associated miR-221. *Cancers*, *12*(1), 27. https://doi.org/10.3390/cancers12010027

Dohrn, M. F., Ihne, S., Hegenbart, U., Medina, J., Zuchner, S. L., Coelho, T., & Hahn, K. (2021). Targeting transthyretin - mechanism-based treatment approaches and future perspectives in hereditary amyloidosis. *Journal of Neurochemistry*, *156*(6), 802–818. https://doi.org/10.1111/jnc.15233

Duncan, D. D., Eshoo, M., Esau, C., Freier, S. M., & Lollo, B. A. (2006). Absolute quantitation of microRNAs with a PCR-based assay. *Analytical Biochemistry*, *359*(2), 268–270. https://doi.org/10.1016/j.ab.2006.08.022

Evans, J. M., & Smitherman, P. (1989). Intratracheal antibiotic treatment. *The Veterinary Record*, *124*(1), 23. https://doi.org/10.1136/vr.124.1.23-a

Eyford, B. A., Singh, C. S. B., Abraham, T., Munro, L., Choi, K. B., Hill, T., Hildebrandt, R., Welch, I., Vitalis, T. Z., Gabathuler, R., Gordon, J. A., Adomat, H., Guns, E. S., Lu, C. J., Pfeifer, C. G., Tian, M. M., & Jefferies, W. A. (2021). A nanomule peptide carrier delivers siRNA across the intact blood-brain barrier to attenuate ischemic stroke. *Frontiers in Molecular Biosciences*, *8*, 611367. https://doi.org/10.3389/fmolb.2021.611367

Ferguson, C. M., Godinho, B. M., Alterman, J. F., Coles, A. H., Hassler, M., Echeverria, D., Gilbert, J. W., Knox, E. G., Caiazzi, J., Haraszti, R. A., King, R. M., Taghian, T., Puri, A., Moser, R. P., Gounis, M. J., Aronin, N., Gray-Edwards, H., & Khvorova, A. (2021). Comparative route of administration studies using therapeutic siRNAs show widespread gene modulation in Dorset sheep. *JCI Insight*, *6*(24). https://doi.org/10.1172/jci.insight.152203

Ferres-Coy, A., Galofre, M., Pilar-Cuellar, F., Vidal, R., Paz, V., Ruiz-Bronchal, E., Campa, L., Pazos, A., Caso, J. R., Leza, J. C., Alvarado, G., Montefeltro, A., Valdizan, E. M., Artigas, F., & Bortolozzi, A. (2016). Therapeutic antidepressant potential of a conjugated siRNA silencing the serotonin transporter after intranasal administration. *Molecular Psychiatry*, *21*(3), 328–338. https://doi.org/10.1038/mp.2015.80

Fowler, M. J., Cotter, J. D., Knight, B. E., Sevick-Muraca, E. M., Sandberg, D. I., & Sirianni, R. W. (2020). Intrathecal drug delivery in the era of nanomedicine. *Advanced Drug Delivery Reviews*, *165–166*, 77–95. https://doi.org/10.1016/j.addr.2020.02.006

Fullana, M. N., Ferres-Coy, A., Ortega, J. E., Ruiz-Bronchal, E., Paz, V., Meana, J. J., Artigas, F., & Bortolozzi, A. (2019). Selective knockdown of TASK3 potassium channel in monoamine neurons: A new therapeutic approach for depression. *Molecular Neurobiology*, *56*(4), 3038–3052. https://doi.org/10.1007/s12035-018-1288-1

Gasca-Salas, C., Fernandez-Rodriguez, B., Pineda-Pardo, J. A., Rodriguez-Rojas, R., Obeso, I., Hernandez-Fernandez, F., del Alamo, M., Mata,

D., Guida, P., Ordas-Bandera, C., Montero-Roblas, J. I., Martinez-Fernandez, R., Foffani, G., Rachmilevitch, I., & Obeso, J. A. (2021). Blood-brain barrier opening with focused ultrasound in Parkinson's disease dementia. *Nature Communications*, *12*(1), 779. https://doi.org/10.1038/s41467-021-21022-9

Geary, R. S. (2009). Antisense oligonucleotide pharmacokinetics and metabolism. *Expert Opinion on Drug Metabolism and Toxicology*, *5*(4), 381–391. https://doi.org/10.1517/17425250902877680

Goebl, N., Berridge, B., Wroblewski, V. J., & Brown-Augsburger, P. L. (2007). Development of a sensitive and specific in situ hybridization technique for the cellular localization of antisense oligodeoxynucleotide drugs in tissue sections. *Toxicologic Pathology*, *35*(4), 541–548. https://doi.org/10.1080/01926230701338958

Goto, A., Yamamoto, S., Igari, T., Matsumoto, S. I., Chisaki, I., Iida, K., Nakayama, M., Oda, A., Kakoi, Y., Uchida, A., Miyata, K., Nishikawa, M., Nagata, T., Kusuhara, H., Yokota, T., & Hirabayashi, H. (2022). Quantitative model analysis and simulation of pharmacokinetics and Malat1 RNA knockdown effect after systemic administration of cholesterol-conjugated DNA/RNA heteroduplex oligonucleotide crossing blood-brain barrier of mice. *Journal of Pharmacology and Experimental Therapeutics*, JPET-AR-2022-001331. https://doi.org/10.1124/jpet.122.001331

Habekost, M., Qvist, P., Denham, M., Holm, I. E., & Jorgensen, A. L. (2021). Directly reprogrammed neurons express MAPT and APP splice variants pertinent to ageing and neurodegeneration. *Molecular Neurobiology*, *58*(5), 2075–2087. https://doi.org/10.1007/s12035-020-02258-w

Hammond, S. M., Abendroth, F., Goli, L., Burrell, M., Thom, G., Gurrell, I., Stoodley, J., Ahlskog, N., Gait, M. J., Wood, M. J. A., & Webster, C. I. (2021). Systemic antibody-oligonucleotide delivery to the central nervous system ameliorates mouse models of spinal muscular atrophy. *bioRxiv preprint*. https://doi.org/10.1101/2021.07.29.454272

Hammond, S. M., Hazell, G., Shabanpoor, F., Saleh, A. F., Bowerman, M., Sleigh, J. N., Meijboom, K. E., Zhou, H., Muntoni, F., Talbot, K., Gait, M. J., & Wood, M. J. (2016). Systemic peptide-mediated oligonucleotide therapy improves long-term survival in spinal muscular atrophy. *Proceedings of the National Academy of Sciences of the United States of America*, *113*(39), 10962–10967. https://doi.org/10.1073/pnas.1605731113

Haroon, M. M., Dar, G. H., Jeyalakshmi, D., Venkatraman, U., Saba, K., Rangaraj, N., Patel, A. B., & Gopal, V. (2016). A designed recombinant fusion protein for targeted delivery of siRNA to the mouse brain. *Journal of Controlled Release*, *228*, 120–131. https://doi.org/10.1016/j.jconrel.2016.03.007

Haroon, M. M., Saba, K., Boddedda, V. H., Kumar, J. M., Patel, A. B., & Gopal, V. (2019). Delivery of BACE1 siRNA mediated by TARBP-BTP fusion protein reduces beta-amyloid deposits in a transgenic mouse model of Alzheimer's disease. *Journal of Biosciences*, *44*(1), 1. https://doi.org/10.1007/s12038-018-9822-x

Hashizume, R., Ozawa, T., Gryaznov, S. M., Bollen, A. W., Lamborn, K. R., Frey, W. H., II, & Deen, D. F. (2008). New therapeutic approach for brain tumors: Intranasal delivery of telomerase inhibitor GRN163. *Neuro-Oncology*, *10*(2), 112–120. https://doi.org/10.1215/15228517-2007-052

He, C., Migawa, M. T., Chen, K., Weston, T. A., Tanowitz, M., Song, W., Guagliardo, P., Iyer, K. S., Bennett, C. F., Fong, L. G., Seth, P. P., Young, S. G., & Jiang, H. (2021). High-resolution visualization and quantification of nucleic acid-based therapeutics in cells and tissues using nanoscale secondary ion mass spectrometry (NanoSIMS). *Nucleic Acids Research*, *49*(1), 1–14. https://doi.org/10.1093/nar/gkaa1112

Herve, F., Ghinea, N., & Scherrmann, J. M. (2008). CNS delivery via adsorptive transcytosis. *The AAPS Journal*, *10*(3), 455–472. https://doi.org/10.1208/s12248-008-9055-2

Hsu, Y., Hettiarachchi, H. D., Zhu, D. C., & Linninger, A. A. (2012). The frequency and magnitude of cerebrospinal fluid pulsations influence intrathecal drug distribution: Key factors for interpatient variability. *Anesthesia & Analgesia*, *115*(2), 386–394. https://doi.org/10.1213/ANE.0b013e3182536211

Hu, P., Zhang, W., Xin, H., & Deng, G. (2016). Single cell isolation and analysis. *Frontiers in Cell and Developmental Biology*, *4*, 116. https://doi.org/10.3389/fcell.2016.00116

Iliff, J. J., Lee, H., Yu, M., Feng, T., Logan, J., Nedergaard, M., & Benveniste, H. (2013). Brain-wide pathway for waste clearance captured by contrast-enhanced MRI. *Journal of Clinical Investigation*, *123*(3), 1299–1309. https://doi.org/10.1172/JCI67677

Iliff, J. J., Wang, M., Liao, Y., Plogg, B. A., Peng, W., Gundersen, G. A., Benveniste, H., Vates, G. E., Deane, R., Goldman, S. A., Nagelhus, E. A., & Nedergaard, M. (2012). A paravascular pathway facilitates CSF flow through the brain parenchyma and the clearance of interstitial solutes, including amyloid beta. *Science Translational Medicine*, *4*(147), 147ra111. https://doi.org/10.1126/scitranslmed.3003748

Jafar-Nejad, P., Powers, B., Soriano, A., Zhao, H., Norris, D. A., Matson, J., DeBrosse-Serra, B., Watson, J., Narayanan, P., Chun, S., Mazur, C., Kordasiewicz, H., Swayze, E. E., & Rigo, F. (2021). The atlas of RNase H antisense oligonucleotide distribution and activity in the CNS of rodents and nonhuman primates following central administration. *Nucleic Acids Research*, *49*(2), 657–673. https://doi.org/10.1093/nar/gkaa1235

Jimenez-Mateos, E. M., Engel, T., Merino-Serrais, P., McKiernan, R. C., Tanaka, K., Mouri, G., Sano, T., O'Tuathaigh, C., Waddington, J. L., Prenter, S., Delanty, N., Farrell, M. A., O'Brien, D. F., Conroy, R. M., Stallings, R. L., DeFelipe, J., & Henshall, D. C. (2012). Silencing microRNA-134 produces neuroprotective and prolonged seizure-suppressive effects. *Nature Medicine*, *18*(7), 1087–1094. https://doi.org/10.1038/nm.2834

Kadry, H., Noorani, B., & Cucullo, L. (2020). A blood-brain barrier overview on structure, function, impairment, and biomarkers of integrity. *Fluids and Barriers of the CNS*, *17*(1), 69. https://doi.org/10.1186/s12987-020-00230-3

Kanazawa, T., Akiyama, F., Kakizaki, S., Takashima, Y., & Seta, Y. (2013). Delivery of siRNA to the brain using a combination of nose-to-brain delivery and cell-penetrating peptide-modified nano-micelles. *Biomaterials*, *34*(36), 9220–9226. https://doi.org/10.1016/j.biomaterials.2013.08.036

Kanazawa, T., Kurano, T., Ibaraki, H., Takashima, Y., Suzuki, T., & Seta, Y. (2019). Therapeutic effects in a transient middle cerebral artery occlusion rat model by nose-to-brain delivery of anti-TNF-alpha siRNA with cell-penetrating peptide-modified polymer micelles. *Pharmaceutics*, *11*(9), 478. https://doi.org/10.3390/pharmaceutics11090478

Kanazawa, T., Morisaki, K., Suzuki, S., & Takashima, Y. (2014). Prolongation of life in rats with malignant glioma by intranasal siRNA/drug codelivery to the brain with cell-penetrating peptide-modified micelles. *Molecular Pharmaceutics*, *11*(5), 1471–1478. https://doi.org/10.1021/mp400644e

Kim, G., Kim, M., Lee, Y., Byun, J. W., Hwang, D. W., & Lee, M. (2020). Systemic delivery of microRNA-21 antisense oligonucleotides to the brain using T7-peptide decorated exosomes. *Journal of Controlled Release*, *317*, 273–281. https://doi.org/10.1016/j.jconrel.2019.11.009

Kimura, S., & Harashima, H. (2020). Current status and challenges associated with CNS-targeted gene delivery across the BBB. *Pharmaceutics*, *12*(12), 1216. https://doi.org/10.3390/pharmaceutics12121216

Korobeynikov, V. A., Lyashchenko, A. K., Blanco-Redondo, B., Jafar-Nejad, P., & Shneider, N. A. (2022). Antisense oligonucleotide silencing of FUS expression as a therapeutic approach in amyotrophic lateral

sclerosis. *Nature Medicine*, *28*(1), 104–116. https://doi.org/10.1038/s41591-021-01615-z

Kumar, P., Wu, H., McBride, J. L., Jung, K. E., Kim, M. H., Davidson, B. L., Kyung Lee, S., Shankar, P., & Manjunath, N. (2007). Transvascular delivery of small interfering RNA to the central nervous system. *Nature*, *448*(7149), 39–43. https://doi.org/10.1038/nature05901

Kuwahara, H., Song, J., Shimoura, T., Yoshida-Tanaka, K., Mizuno, T., Mochizuki, T., Zeniya, S., Li, F., Nishina, K., Nagata, T., Ito, S., Kusuhara, H., & Yokota, T. (2018). Modulation of blood-brain barrier function by a heteroduplex oligonucleotide in vivo. *Scientific Reports*, *8*(1), 4377. https://doi.org/10.1038/s41598-018-22577-2

Landesman, Y., Svrzikapa, N., Cognetta, A., III, Zhang, X., Bettencourt, B. R., Kuchimanchi, S., Dufault, K., Shaikh, S., Gioia, M., Akinc, A., Hutabarat, R., & Meyers, R. (2010). In vivo quantification of formulated and chemically modified small interfering RNA by heating-in-Triton quantitative reverse transcription polymerase chain reaction (HIT qRT-PCR). *Silence*, *1*(1), 16. https://doi.org/10.1186/1758-907X-1-16

Li, P., Gong, Y., Kim, J., Liu, X., Gilbert, J., Kerns, H. M., Groth, R., & Rooney, M. (2020). Hybridization liquid chromatography-tandem mass spectrometry: An alternative bioanalytical method for antisense oligonucleotide quantitation in plasma and tissue samples. *Analytical Chemistry*, *92*(15), 10548–10559. https://doi.org/10.1021/acs.analchem.0c01382

Lin, Z. J., Li, W., & Dai, G. (2007). Application of LC-MS for quantitative analysis and metabolite identification of therapeutic oligonucleotides. *Journal of Pharmaceutical and Biomedical Analysis*, *44*(2), 330–341. https://doi.org/10.1016/j.jpba.2007.01.042

Linnane, E., Davey, P., Zhang, P., Puri, S., Edbrooke, M., Chiarparin, E., Revenko, A. S., Macleod, A., Norman, J. C., & Ross, S. J. (2019). Differential uptake, kinetics and mechanisms of intracellular trafficking of next-generation antisense oligonucleotides across human cancer cell lines. *Nucleic Acids Research*, *47*(9), 4375–4392. https://doi.org/10.1093/nar/gkz214

Louveau, A., Smirnov, I., Keyes, T. J., Eccles, J. D., Rouhani, S. J., Peske, J. D., Derecki, N. C., Castle, D., Mandell, J. W., Lee, K. S., Harris, T. H., & Kipnis, J. (2016). Corrigendum: Structural and functional features of central nervous system lymphatic vessels. *Nature*, *533*(7602), 278. https://doi.org/10.1038/nature16999

Ma, Q., Dasgupta, C., Li, Y., Bajwa, N. M., Xiong, F., Harding, B., Hartman, R., & Zhang, L. (2016). Inhibition of microRNA-210 provides neuroprotection in hypoxic-ischemic brain injury in neonatal rats. *Neurobiology of Disease*, *89*, 202–212. https://doi.org/10.1016/j.nbd.2016.02.011

Mahajan, S., Zhao, H., Kovacina, K., Lachacz, E., Hoxha, S., Chan, J., & Liang, M. (2022). High-sensitivity quantification of antisense oligonucleotides for pharmacokinetic characterization. *Bioanalysis*, *14*(9), 603–613. https://doi.org/10.4155/bio-2022-0035

Mainprize, T., Lipsman, N., Huang, Y., Meng, Y., Bethune, A., Ironside, S., Heyn, C., Alkins, R., Trudeau, M., Sahgal, A., Perry, J., & Hynynen, K. (2019). Blood-brain barrier opening in primary brain tumors with noninvasive MR-guided focused ultrasound: A clinical safety and feasibility study. *Scientific Reports*, *9*(1), 321. https://doi.org/10.1038/s41598-018-36340-0

Marx, D., Williams, G., & Birkhoff, M. (2015). Intranasal drug administration—An attractive delivery route for some drugs. *Drug Discovery and Development*. https://doi.org/10.5772/59468

Mazur, C., Powers, B., Zasadny, K., Sullivan, J. M., Dimant, H., Kamme, F., Hesterman, J., Matson, J., Oestergaard, M., Seaman, M., Holt, R. W., Qutaish, M., Polyak, I., Coelho, R., Gottumukkala, V., Gaut, C. M., Berridge, M., Albargothy, N. J., Kelly, L., … Verma, A. (2019). Brain pharmacology of intrathecal antisense oligonucleotides revealed through multimodal imaging. *JCI Insight*, *4*(20). https://doi.org/10.1172/jci.insight.129240

Mendonca, M. C. P., Kont, A., Aburto, M. R., Cryan, J. F., & O'Driscoll, C. M. (2021). Advances in the design of (nano)formulations for delivery of antisense oligonucleotides and small interfering RNA: Focus on the central nervous system. *Molecular Pharmaceutics*, *18*(4), 1491–1506. https://doi.org/10.1021/acs.molpharmaceut.0c01238

Mestre, H., Mori, Y., & Nedergaard, M. (2020). The brain's glymphatic system: Current controversies. *Trends in Neurosciences*, *43*(7), 458–466. https://doi.org/10.1016/j.tins.2020.04.003

Miller, T. M., Cudkowicz, M. E., Genge, A., Shaw, P. J., Sobue, G., Bucelli, R. C., Chio, A., Van Damme, P., Ludolph, A. C., Glass, J. D., Andrews, J. A., Babu, S., Benatar, M., McDermott, C. J., Cochrane, T., Chary, S., Chew, S., Zhu, H., Wu, F., … OLE Working Group. (2022). Trial of antisense oligonucleotide Tofersen for SOD1 ALS. *New England Journal of Medicine*, *387*(12), 1099–1110. https://doi.org/10.1056/NEJMoa2204705

Miller, T. M., Pestronk, A., David, W., Rothstein, J., Simpson, E., Appel, S. H., Andres, P. L., Mahoney, K., Allred, P., Alexander, K., Ostrow, L. W., Schoenfeld, D., Macklin, E. A., Norris, D. A., Manousakis, G., Crisp, M., Smith, R., Bennett, C. F., Bishop, K. M., … Cudkowicz, M. E. (2013). An antisense oligonucleotide against SOD1 delivered intrathecally for patients with SOD1 familial amyotrophic lateral sclerosis: A phase 1, randomised, first-in-man study. *The Lancet Neurology*, *12*(5), 435–442. https://doi.org/10.1016/S1474-4422(13)70061-9

Min, H. S., Kim, H. J., Naito, M., Ogura, S., Toh, K., Hayashi, K., Kim, B. S., Fukushima, S., Anraku, Y., Miyata, K., & Kataoka, K. (2020). Systemic brain delivery of antisense oligonucleotides across the blood-brain barrier with a glucose-coated polymeric nanocarrier. *Angewandte Chemie International Edition in English*, *59*(21), 8173–8180. https://doi.org/10.1002/anie.201914751

Monine, M., Norris, D., Wang, Y., & Nestorov, I. (2021). A physiologically-based pharmacokinetic model to describe antisense oligonucleotide distribution after intrathecal administration. *Journal of Pharmacokinetics and Pharmacodynamics*, *48*(5), 639–654. https://doi.org/10.1007/s10928-021-09761-0

Mukashyaka, M. C., Wu, C. L., Ha, K., Zhang, J., Wood, J., Foley, S., Mastis, B., Jungels, N., Sun, H., Shadid, M., Harriman, S., & Hadcock, J. R. (2021). Pharmacokinetic/pharmacodynamic modeling of a cell-penetrating peptide phosphorodiamidate morpholino oligomer in mdx mice. *Pharmaceutical Research*, *38*(10), 1731–1745. https://doi.org/10.1007/s11095-021-03118-5

Mullard, A. (2022). Antibody-oligonucleotide conjugates enter the clinic. *Nature Reviews Drug Discovery*, *21*(1), 6–8. https://doi.org/10.1038/d41573-021-00213-5

Nagata, T., Dwyer, C. A., Yoshida-Tanaka, K., Ihara, K., Ohyagi, M., Kaburagi, H., Miyata, H., Ebihara, S., Yoshioka, K., Ishii, T., Miyata, K., Miyata, K., Powers, B., Igari, T., Yamamoto, S., Arimura, N., Hirabayashi, H., Uchihara, T., Hara, R. I., … Yokota, T. (2021). Cholesterol-functionalized DNA/RNA heteroduplexes cross the blood-brain barrier and knock down genes in the rodent CNS. *Nature Biotechnology*, *39*(12), 1529–1536. https://doi.org/10.1038/s41587-021-00972-x

Nakada-Honda, N., Cui, D., Matsuda, S., & Ikeda, E. (2021). Intravenous injection of cyclophilin A realizes the transient and reversible opening of barrier of neural vasculature through basigin in endothelial cells. *Scientific Reports*, *11*(1), 19391. https://doi.org/10.1038/s41598-021-98163-w

Negishi, Y., Yamane, M., Kurihara, N., Endo-Takahashi, Y., Sashida, S., Takagi, N., Suzuki, R., & Maruyama, K. (2015). Enhancement of blood-brain barrier permeability and delivery of antisense oligonucleotides or plasmid DNA to the brain by the combination of bubble liposomes and high-intensity focused ultrasound. *Pharmaceutics*, *7*(3), 344–362. https://doi.org/10.3390/pharmaceutics7030344

Nott, A., Schlachetzki, J. C. M., Fixsen, B. R., & Glass, C. K. (2021). Nuclei isolation of multiple brain cell types for omics interrogation. *Nature*

Protocols, *16*(3), 1629–1646. https://doi.org/10.1038/s41596-020-00472-3

Nuckowski, L., Kaczmarkiewicz, A., & Studzinska, S. (2018). Review on sample preparation methods for oligonucleotides analysis by liquid chromatography. *Journal of Chromatography, B: Analytical Technologies in the Biomedical and Life Sciences*, *1090*, 90–100. https://doi.org/10.1016/j.jchromb.2018.05.025

O'Reilly, M. A., Hough, O., & Hynynen, K. (2017). Blood-brain barrier closure time after controlled ultrasound-induced opening is independent of opening volume. *Journal of Ultrasound in Medicine*, *36*(3), 475–483. https://doi.org/10.7863/ultra.16.02005

Ovsepian, S. V., Bodeker, M., O'Leary, V. B., Lawrence, G. W., & Oliver Dolly, J. (2015). Internalization and retrograde axonal trafficking of tetanus toxin in motor neurons and trans-synaptic propagation at central synapses exceed those of its C-terminal-binding fragments. *Brain Structure and Function*, *220*(3), 1825–1838. https://doi.org/10.1007/s00429-015-1004-0

Patel, M. M., & Patel, B. M. (2017). Crossing the blood-brain barrier: Recent advances in drug delivery to the brain. *CNS Drugs*, *31*(2), 109–133. https://doi.org/10.1007/s40263-016-0405-9

Pendergraff, H., Schmidt, S., Vikesa, J., Weile, C., Overup, C., W. Lindholm, M., & Koch, T. (2020). Nuclear and cytoplasmatic quantification of unconjugated, label-free locked nucleic acid oligonucleotides. *Nucleic Acid Therapeutics*, *30*(1), 4–13. https://doi.org/10.1089/nat.2019.0810

Penichet, M. L., Kang, Y. S., Pardridge, W. M., Morrison, S. L., & Shin, S. U. (1999). An antibody-avidin fusion protein specific for the transferrin receptor serves as a delivery vehicle for effective brain targeting: Initial applications in anti-HIV antisense drug delivery to the brain. *Journal of Immunology*, *163*(8), 4421–4426.

Plog, B. A., Dashnaw, M. L., Hitomi, E., Peng, W., Liao, Y., Lou, N., Deane, R., & Nedergaard, M. (2015). Biomarkers of traumatic injury are transported from brain to blood via the glymphatic system. *Journal of Neuroscience*, *35*(2), 518–526. https://doi.org/10.1523/JNEUROSCI.3742-14.2015

Pulgar, V. M. (2018). Transcytosis to cross the blood brain barrier, new advancements and challenges. *Frontiers in Neuroscience*, *12*, 1019. https://doi.org/10.3389/fnins.2018.01019

Robin, V., Griffith, G., Carter, J. L., Leumann, C. J., Garcia, L., & Goyenvalle, A. (2017). Efficient SMN rescue following subcutaneous tricyclo-DNA antisense oligonucleotide treatment. *Molecular Therapy - Nucleic Acids*, *7*, 81–89. https://doi.org/10.1016/j.omtn.2017.02.009

Sanchez-Ramos, J., Song, S., Kong, X., Foroutan, P., Martinez, G., Dominguez-Viqueria, W., Mohapatra, S., Mohapatra, S., Haraszti, R. A., Khvorova, A., Aronin, N., & Sava, V. (2018). Chitosan-Mangafodipir nanoparticles designed for intranasal delivery of siRNA and DNA to brain. *Journal of Drug Delivery Science and Technology*, *43*, 453–460. https://doi.org/10.1016/j.jddst.2017.11.013

Sava, V., Fihurka, O., Khvorova, A., & Sanchez-Ramos, J. (2020). Enriched chitosan nanoparticles loaded with siRNA are effective in lowering Huntington's disease gene expression following intranasal administration. *Nanomedicine: Nanotechnology, Biology and Medicine*, *24*, 102119. https://doi.org/10.1016/j.nano.2019.102119

Shabanpoor, F., Hammond, S. M., Abendroth, F., Hazell, G., Wood, M. J. A., & Gait, M. J. (2017). Identification of a peptide for systemic brain delivery of a morpholino oligonucleotide in mouse models of spinal muscular atrophy. *Nucleic Acid Therapeutics*, *27*(3), 130–143. https://doi.org/10.1089/nat.2016.0652

Sharp, M. K., Diem, A. K., Weller, R. O., & Carare, R. O. (2016). Peristalsis with oscillating flow resistance: A mechanism for periarterial clearance of amyloid beta from the brain. *Annals of Biomedical Engineering*, *44*(5), 1553–1565. https://doi.org/10.1007/s10439-015-1457-6

Shi, J., Chen, X., Diao, J., Jiang, L., Li, L., Li, S., Liang, W., Jin, X., Wang, Y., Wong, C., Zhang, X. T., & Tse, F. L. S. (2021). Bioanalysis in the age of new drug modalities. *The AAPS Journal*, *23*(3), 64. https://doi.org/10.1208/s12248-021-00594-w

Shi, R., Sun, Y. H., Zhang, X. H., & Chiang, V. L. (2012). Poly(T) adaptor RT-PCR. *Methods in Molecular Biology*, *822*, 53–66. https://doi.org/10.1007/978-1-61779-427-8_4

Spencer, B., Trinh, I., Rockenstein, E., Mante, M., Florio, J., Adame, A., El-Agnaf, O. M., Kim, C., Masliah, E., & Rissman, R. A. (2019). Systemic peptide mediated delivery of an siRNA targeting alpha-syn in the CNS ameliorates the neurodegenerative process in a transgenic model of Lewy body disease. *Neurobiology of Disease*, *127*, 163–177. https://doi.org/10.1016/j.nbd.2019.03.001

Stratford, S., Stec, S., Jadhav, V., Seitzer, J., Abrams, M., & Beverly, M. (2008). Examination of real-time polymerase chain reaction methods for the detection and quantification of modified siRNA. *Analytical Biochemistry*, *379*(1), 96–104. https://doi.org/10.1016/j.ab.2008.05.001

Studzinska, S. (2018). Review on investigations of antisense oligonucleotides with the use of mass spectrometry. *Talanta*, *176*, 329–343. https://doi.org/10.1016/j.talanta.2017.08.025

Sullivan, J. M., Mazur, C., Wolf, D. A., Horky, L., Currier, N., Fitzsimmons, B., Hesterman, J., Pauplis, R., Haller, S., Powers, B., Tayefeh, L., DeBrosse-Serra, B., Hoppin, J., Kordasiewicz, H., Swayze, E. E., & Verma, A. (2020). Convective forces increase rostral delivery of intrathecal radiotracers and antisense oligonucleotides in the cynomolgus monkey nervous system. *Journal of Translational Medicine*, *18*(1), 309. https://doi.org/10.1186/s12967-020-02461-2

Sweeney, M. D., Zhao, Z., Montagne, A., Nelson, A. R., & Zlokovic, B. V. (2019). Blood-brain barrier: From physiology to disease and back. *Physiological Reviews*, *99*(1), 21–78. https://doi.org/10.1152/physrev.00050.2017

Syed, Y. Y. (2021). Givosiran: A review in acute hepatic porphyria. *Drugs*, *81*(7), 841–848. https://doi.org/10.1007/s40265-021-01511-3

Szentistvanyi, I., Patlak, C. S., Ellis, R. A., & Cserr, H. F. (1984). Drainage of interstitial fluid from different regions of rat brain. *American Journal of Physiology*, *246*(6 Pt 2), F835–F844. https://doi.org/10.1152/ajprenal.1984.246.6.F835

Tabrizi, S. J., Leavitt, B. R., Landwehrmeyer, G. B., Wild, E. J., Saft, C., Barker, R. A., Blair, N. F., Craufurd, D., Priller, J., Rickards, H., Rosser, A., Kordasiewicz, H. B., Czech, C., Swayze, E. E., Norris, D. A., Baumann, T., Gerlach, I., Schobel, S. A., Paz, E., … Phase 1–2a IONIS-HTTRx Study Site Teams. (2019). Targeting huntingtin expression in patients with Huntington's disease. *New England Journal of Medicine*, *380*(24), 2307–2316. https://doi.org/10.1056/NEJMoa1900907

Thayer, M. B., Lade, J. M., Doherty, D., Xie, F., Basiri, B., Barnaby, O. S., Bala, N. S., & Rock, B. M. (2019). Application of locked nucleic acid oligonucleotides for siRNA preclinical bioanalytics. *Scientific Reports*, *9*(1), 3566. https://doi.org/10.1038/s41598-019-40187-4

Uchida, A., Goto, R., Usui, T., Tachikawa, M., & Terasaki, T. (2022). Blood-arachnoid barrier as a dynamic physiological and pharmacological interface between cerebrospinal fluid and blood. In E. C. M. de Lange, M. Hammarlund-Udenaes, & R. G. Thorne (Eds.), *Drug delivery to the brain* (pp. 93–121). Springer Cham. https://doi.org/10.1007/978-3-030-88773-5_4

Ueda, H. R., Erturk, A., Chung, K., Gradinaru, V., Chedotal, A., Tomancak, P., & Keller, P. J. (2020). Tissue clearing and its applications in neuroscience. *Nature Reviews Neuroscience*, *21*(2), 61–79. https://doi.org/10.1038/s41583-019-0250-1

Valenzuela, A., Tardiveau, C., Ayuso, M., Buyssens, L., Bars, C., Van Ginneken, C., Fant, P., Leconte, I., Braendli-Baiocco, A., Parrott, N., Schmitt, G., Tessier, Y., Barrow, P., & Van Cruchten, S. (2021). Safety testing of an antisense oligonucleotide intended for pediatric indications in the Juvenile Gottingen Minipig, including an evaluation of the ontogeny of key nucleases. *Pharmaceutics*, *13*(9), 1442. https://doi.org/10.3390/pharmaceutics13091442

Wang, Z., Xiong, G., Tsang, W. C., Schatzlein, A. G., & Uchegbu, I. F. (2019). Nose-to-brain delivery. *Journal of Pharmacology and Experimental*

Therapeutics, *370*(3), 593–601. https://doi.org/10.1124/jpet.119.258152

Webster, C. I., Hatcher, J., Burrell, M., Thom, G., Thornton, P., Gurrell, I., & Chessell, I. (2017). Enhanced delivery of IL-1 receptor antagonist to the central nervous system as a novel anti-transferrin receptor-IL-1RA fusion reverses neuropathic mechanical hypersensitivity. *Pain*, *158*(4), 660–668. https://doi.org/10.1097/j.pain.0000000000000810

Wei, X., Dai, G., Marcucci, G., Liu, Z., Hoyt, D., Blum, W., & Chan, K. K. (2006). A specific picomolar hybridization-based ELISA assay for the determination of phosphorothioate oligonucleotides in plasma and cellular matrices. *Pharmaceutical Research*, *23*(6), 1251–1264. https://doi.org/10.1007/s11095-006-0082-3

Wolf, D. A., Hesterman, J. Y., Sullivan, J. M., Orcutt, K. D., Silva, M. D., Lobo, M., Wellman, T., Hoppin, J., & Verma, A. (2016). Dynamic dual-isotope molecular imaging elucidates principles for optimizing intrathecal drug delivery. *JCI Insight*, *1*(2), e85311. https://doi.org/10.1172/jci.insight.85311

Wu, S. K., Tsai, C. L., Huang, Y., & Hynynen, K. (2020). Focused ultrasound and microbubbles-mediated drug delivery to brain tumor. *Pharmaceutics*, *13*(1), 15. https://doi.org/10.3390/pharmaceutics13010015

Wu, T. T., Su, F. J., Feng, Y. Q., Liu, B., Li, M. Y., Liang, F. Y., Li, X. j., Zhang, Y., Cai, Z. q., & Pei, Z. (2020). Mesenchymal stem cells alleviate AQP-4-dependent glymphatic dysfunction and improve brain distribution of antisense oligonucleotides in BACHD mice. *Stem Cells*, *38*(2), 218–230. https://doi.org/10.1002/stem.3103

Xie, L., Kang, H., Xu, Q., Chen, M. J., Liao, Y., Thiyagarajan, M., O'Donnell, J., Christensen, D. J., Nicholson, C., Iliff, J. J., Takano, T., Deane, R., & Nedergaard, M. (2013). Sleep drives metabolite clearance from the adult brain. *Science*, *342*(6156), 373–377. https://doi.org/10.1126/science.1241224

Yang, Y., Zhang, X., Wu, S., Zhang, R., Zhou, B., Zhang, X., Tang, L., Tian, Y., Men, K., & Yang, L. (2022). Enhanced nose-to-brain delivery of siRNA using hyaluronan-enveloped nanomicelles for glioma therapy. *Journal of Controlled Release*, *342*, 66–80. https://doi.org/10.1016/j.jconrel.2021.12.034

Yu, R. Z., Baker, B., Chappell, A., Geary, R. S., Cheung, E., & Levin, A. A. (2002). Development of an ultrasensitive noncompetitive hybridization-ligation enzyme-linked immunosorbent assay for the determination of phosphorothioate oligodeoxynucleotide in plasma. *Analytical Biochemistry*, *304*(1), 19–25. https://doi.org/10.1006/abio.2002.5576

Yuan, Z., Zhao, L., Zhang, Y., Li, S., Pan, B., Hua, L., Wang, Z., Ye, C., Lu, J., Yu, R., & Liu, H. (2018). Inhibition of glioma growth by a GOLPH3 siRNA-loaded cationic liposomes. *Journal of Neuro-Oncology*, *140*(2), 249–260. https://doi.org/10.1007/s11060-018-2966-6

Zeniya, S., Kuwahara, H., Daizo, K., Watari, A., Kondoh, M., Yoshida-Tanaka, K., Kaburagi, H., Asada, K., Nagata, T., Nagahama, M., Yagi, K., & Yokota, T. (2018). Angubindin-1 opens the blood-brain barrier in vivo for delivery of antisense oligonucleotide to the central nervous system. *Journal of Controlled Release*, *283*, 126–134. https://doi.org/10.1016/j.jconrel.2018.05.010

Zhang, G., Lin, J., Srinivasan, K., Kavetskaia, O., & Duncan, J. N. (2007). Strategies for bioanalysis of an oligonucleotide class macromolecule from rat plasma using liquid chromatography-tandem mass spectrometry. *Analytical Chemistry*, *79*(9), 3416–3424. https://doi.org/10.1021/ac0618674

Zhang, J., Li, Z., Wang, H., Wang, Y., Jia, H., & Yan, J. (2011). Ultrasensitive quantification of mature microRNAs by real-time PCR based on ligation of a ribonucleotide-modified DNA probe. *Chemical Communications*, *47*(33), 9465–9467. https://doi.org/10.1039/c1cc13466c

Zhang, L., Wu, T., Shan, Y., Li, G., Ni, X., Chen, X., Hu, X., Lin, L., Guan, Y., Gao, J., Chen, D., Zhang, Y., Pei, Z., & Chen, X. (2021). Therapeutic reversal of Huntington's disease by in vivo self-assembled siRNAs. *Brain*, *144*(11), 3421–3435. https://doi.org/10.1093/brain/awab354

How to cite this article: Goto, A., Yamamoto, S., & Iwasaki, S. (2023). Biodistribution and delivery of oligonucleotide therapeutics to the central nervous system: Advances, challenges, and future perspectives. *Biopharmaceutics and Drug Disposition*, *44*(1), 26–47. https://doi.org/10.1002/bdd.2338